2015

A Real-Time Signal Control System to Minimize Emissions at Isolated Intersections

Farnoush Khalighi

A REAL-TIME SIGNAL CONTROL SYSTEM TO MINIMIZE EMISSIONS AT ISOLATED INTERSECTIONS

A Thesis Presented

by

FARNOUSH KHALIGHI

Submitted to the Graduate School of the
University of Massachusetts Amherst in partial fulfillment
of the requirements for the degree of

MASTER OF SCIENCE

May, 2015

Civil and Environmental Engineering Department

A REAL-TIME SIGNAL CONTROL SYSTEM TO MINIMIZE EMISSIONS AT ISOLATED INTERSECTIONS

A Thesis Presented

by

FARNOUSH KHALIGHI

Approved as to style and content by:

Eleni Christofa, Chair

Eric J. Gonzales, Member

Daiheng Ni, Member

Richard N. Palmer, Department Chair
Civil and Environmental Engineering Department

ACKNOWLEDGMENTS

I would like to express my sincere gratitude to my adviser Dr. Eleni Christofa for the continuous support of my study and research, for her patience, motivation, and immense knowledge. Her guidance helped me in all the time of research and writing this thesis.

Besides, I would like to thank the rest of my thesis committee, Dr. Daiheng Ni and Dr. Eric Gonzales, for their insightful comments and useful questions.

ABSTRACT

A REAL-TIME SIGNAL CONTROL SYSTEM TO MINIMIZE EMISSIONS AT ISOLATED INTERSECTIONS

MAY, 2015

FARNOUSH KHALIGHI

M.S., UNIVERSITY OF MASSACHUSETTS AMHERST

Directed by: Professor Eleni Christofa

Continuous transportation demand growth in recent years has led to many traffic issues in urban areas. Among the most challenging ones are traffic congestion and the associated vehicular emissions. Efficient design of traffic signal control systems can be a promising approach to address these problems. This research develops a real-time signal control system, which optimizes signal timings at an under-saturated isolated intersection by minimizing total vehicular emissions. A combination of previously introduced analytical models based on traffic flow theory have been used. These models are able to estimate time spent per driving mode (i.e., time spent accelerating, decelerating, cruising, and idling) as a function of demand, vehicle arrival times, saturation flow, and signal control parameters. Information on vehicle activity is used along with the Vehicle Specific Power (VSP) model, which estimates emission rates per time spent in each operating mode to obtain total emissions per cycle. For the evaluation of the proposed method, data from two real-world intersections of Mesogion and Katechaki Avenues located in Athens, Greece and University and San Pablo

Avenues, in Berkeley, CA has been used used. The evaluation has been performed through both deterministic (i.e. under the assumption of perfect information for all inputs) and stochastic (i.e. without having perfect information for some inputs) arrival tests. The results of evaluation tests has shown that the proposed emission-based signal control system reduces emissions compared to traditional vehicle-based signal control system in most cases.

TABLE OF CONTENTS

LIST OF TABLES

Table **Page**

LIST OF FIGURES

Figure **Page**

CHAPTER 1

INTRODUCTION

Increases in traffic congestion caused by growth in population and car ownership threaten mobility and quality of life in populated cities around the world. Traffic congestion is directly associated with reduced mobility as well as increased wasted time, fuel consumption, and pollutant emissions. Particularly, in urban areas motor operations have a huge contribution to increasing level of air pollutants such as CO_2, CO, HC, and NO_x. Among the traffic-generated air pollutants emitted by vehicles near intersections, NO_x is of great importance. Current scientific evidence links short-term NO_2 exposure, ranging from 30 minutes to 24 hours, with adverse respiratory effects including airway inflammation in healthy humans and increased respiratory symptoms in people with asthma (EPA, 2015). Furthermore, other studies show that motor vehicles are responsible for 57% of NO_x emissions in the United States (Black, 1942).

Reducing congestion by adding new roads is not always feasible because of spatial and financial constraints. This is particularly hard in the United States that funding surface transportation has been faced with some difficulties in recent years (Dilger, 2002). Additionally, a significant amount of emissions is usually produced during the construction process. Furthermore, increasing road capacity could result in increased future demand, so not only it cannot reduce congestion in the long run but it can lead to worse emission inventories. Therefore, employing another method to deal with the problem of reducing emissions and at the same time maintaining efficient and reliable traffic operations is necessary. Traffic signals, if controlled appropriately,

can be promising tools for improving traffic conditions, since they can be implemented using existing infrastructure and do not need large investments.

Signal control systems have been traditionally designed to reduce travel time or vehicle delay at intersections. However, recently with increased requirements and emission standards, a lot of attention has been attracted to evaluating the environmental impacts of signal control strategies and developing methods to estimate and reduce emissions at intersections. Studies show that minimizing delay does not necessarily result in reduced emissions. The main reason for high emission levels at urban intersections is non-smooth traffic operations and stop-and-go vehicle movements (Chen and Yu, 2007). Highly interrupted movements of vehicles result in much more time spent in the acceleration mode. During acceleration, a vehicle's engine power is at a higher level, and it causes excessive fuel consumption and emissions (Frey et al., 2000). Therefore, to minimize emissions, the emissions should be taken into account directly when optimizing signal timings.

1.1 Problem Statement

There have been studies on emission estimation and the impact of signal timings on emissions at signalized intersections. Most of these studies have been performed through field measurements or simulation software. However, estimating emissions through simulation studies and field measurements is not always efficient and even feasible since they are time-consuming and in some cases prohibitively expensive. Therefore, there is an imperative need to develop real-time signal control systems to estimate emissions with minimum inputs and use these estimates to develop real-time signal control systems to improve air quality. In addition, in such real-time signal control systems, it is necessary to account for emissions produced by both autos and transit vehicles at multimodal signalized intersections since the amount of emissions

produced by autos and transit vehicles are considerably different due to the higher emission rates of transit vehicles.

So, the question that motivates this research is the following:

How should real-time signal control systems be designed to minimize emissions at signalized intersections, accounting for emissions produced by both autos and transit vehicles?

1.2 Research Goals

This study has develop ed a real-time signal control strategy to minimize emissions at an isolated intersection that operates at undersaturated traffic conditions.

The proposed system first predicts the time spent on each operation mode: acceleration, deceleration, cruising, and idling for both autos and transit vehicles with the use of previously develop ed analytical models (Christofa et al., 2013, Shabihkhani and Gonzales, 2013). Then, information on time spent p er driving mode is used along with modal emission rates to estimate total emission levels. Then the total emissions is minimized through optimizing signal timings. The proposed real-time signal control strategy has been tested through deterministic (i.e., under the assumption of perfect information ab out auto and transit vehicle arrivals) and stochastic (i.e., when perfect information is not available for auto and transit vehicle arrivals) arrival tests at two real-world intersections that vary in their geometric as well as traffic and transit characteristics.

CHAPTER 2

LITERATURE REVIEW

Extensive literature exists on the environmental impacts of signal control strategies. Traditionally, traffic signals have been designed to improve traffic congestion, delay, travel time, and vehicles' speed. However, in recent years investigating and studying the environmental effects of traffic control strategies has attracted lots of attention in response to growing restricted emission standards for transportation projects. Considering the need to estimate vehicular emissions, several studies have been performed and a number of emission models have been developed. These studies can be categorized into three groups of field measurements, simulation studies, and analytical studies based upon their approach to estimate emissions. Furthermore, a number of emission models have been developed, which can be integrated within traffic simulation models to provide estimates of emission inventories based on vehicles' activities.

This chapter presents models and methods that have been developed to estimate vehicle emissions in addition to signal timing optimization systems that aim at reducing emissions at signalized intersections.

2.1 Vehicle Emission Estimation

The environmental impacts of transportation have always been important to transportation professionals. According to the Clean Air Act Amendments (CAAA) in 1990, emission estimates had to be provided for any proposed traffic improvement project (Rakha et al., 2004a).

Traditionally, signal control strategies have been designed such that they reduce delay. However, reducing delay does not necessarily result in fewer emissions and fuel consumption. Several studies have indicated that higher emission levels are produced in operation modes that cause higher engine power. The acceleration mode contributes most to emissions production because of the higher vehicle's engine power associated with this mode (Frey et al., 2000). Accelerations occur after each stop, so the number of stops is a key factor in estimating emissions (Barth and Boriboonsomsin, 2008). Considering the need to estimate vehicular emissions, several models have been developed and studies have been performed. The models are aimed to estimating emissions as functions of certain inputs. The studies that have evaluated the impact of traffic operations and signal control on emissions can be categorized into three groups of field measurements, simulation studies, and analytical studies based on their approach for estimating emissions.

2.1.1 Vehicle Emission Models

Many traffic operations software packages include an emission model to assess the emission levels resulting from traffic operations. Emission models utilized within traffic models are typically developed based on laboratory dynamometer tests. In dynamometer tests, standardized driving cycles under controlled ambient conditions are defined. Each driving cycle is characterized by an overall average speed, and has a unique profile of stops, starts, cruises, accelerations, and decelerations.

In response to the need for estimating emissions several emission models have been developed. A number of vehicle emission models were developed by the U.S. Environmental Protection Agency (EPA) such as the mobile source emission factor model (MOBILE), and the California Air Resources Board (CARB) like the EMission FACtors (EMFAC). However, these models were not designed to estimate emissions of operational-level projects such as traffic signal coordination, ramp metering, and

other Intelligent Transportation System (ITS) strategies. Therefore, developing a tool, which can predict the environmental impacts of operational-level projects was necessary (Rakha et al., 2004a). The Multi-Scale Motor Vehicle and Equipment Emission System (MOVES), the Comprehensive Modal Emission Model (CMEM), and the VT-Micro are examples of models, which have made operational-level emission estimation possible. All these models are described in greater detail in the next sections.

Mobile Source Emission Factor Model (MOBILE)

MOBILE is one of the first emission estimation models, which provides emission estimates for highway motor vehicles. MOBILE is a macroscopic emission model that calculates emissions as a function of aggregate parameters like average speed and vehicle miles traveled (VMT). Therefore, it cannot give valuable emission estimates for traffic control projects, which affect changes in speed but not necessarily the average speed. Due to this shortcoming it has not been integrated with a lot of traffic simulation software packages (Rouphail et al., 2001).

The MOBILE emission model has been updated periodically and older versions have been replaced by newer ones. So far, six different versions of MOBILE (MOBILE1 to MOBILE6) have been developed from 1978 to 2002. Each new version has been developed by collecting and analyzing new test data, and accounting for changes in vehicle types, engine, emission control system technologies, and emission standards. MOBILE6 is the latest version of this model released in 2002. It is capable of providing estimates for a wide variety of pollutants including hydrocarbons (HC), carbon monoxide (CO), oxides of nitrogen (NO_x), exhaust particulate matter, tire wear particulate matter, break wear particulate matter, sulfur oxide (SO_2), and carbon dioxide (CO_2) (Koupal et al., 2003).

The main disadvantage of MOBILE is that it only estimates emissions in large scale and is not able to predict the environmental impacts of operational-level projects

(Rakha et al., 2004a).

EMission FACtors (EMFAC)

EMFAC is a mobile source emission model approved for California. It was developed by the California Air Resources Board (CARB). Similar to the MOBILE emission model, EMFAC is a macroscopic model and uses only average speed as the primary descriptor of a vehicle's driving cycle to estimate exhaust emissions. Without taking speed changes into account, average speed-based methods may inaccurately estimate emissions from actual driving behavior. Hence, EMFAC and MOBILE are not capable of accounting for different emissions rates for the four operating modes: acceleration, deceleration, cruising, and idling (Bai et al., 2009).

EMFAC2011 is the latest version of this model, which was released in response to the new requirements of the Federal Highway Administration for presenting emission estimates of proposed traffic projects. EMFAC2011 includes the latest data on California's car and truck fleets and travel activity. In order to incorporate new data for emission estimation of diesel trucks and buses, a modular emission modeling approach was used in the development of EMFAC2011. EMFAC2011 has three modules: 1) EMFAC-LDV, which estimates emissions of passenger vehicles. This module is used for estimating the emissions from gasoline powered on-road vehicles, diesel vehicles with a gross vehicle weight lower than 14,000 pounds, and urban transit buses; 2) EMFAC-HD that estimates emissions from diesel trucks and buses. This module is used for estimating emissions of diesel trucks and buses with a gross vehicle weight greater than 14,000 pounds; and 3) EMFAC-SG that integrates the output of EMFAC-LDV and EMFAC-HD and applies scaling factors to estimate emissions consistent with user-defined VMT and speeds. EMFAC provides users with the ability to perform scenario assessments for transportation planning projects in terms of

emission production.

Multi-Scale Motor Vehicle and Equipment Emission System (MOVES)

MOVES is a microscopic emission model developed by EPA. Before developing MOVES, EPA's emission estimation tools and underlying emission factors were calculated as functions of average vehicles' operating characteristics such as average travel speed and VMT for broad geographical areas (e.g., nationwide scale) nationwide scale to assess overall trends. However, in recent years needs to assess the environmental impacts of operational-level projects have led to the development of finer-scale modeling approaches. In the development of modal emission rates for MOVES different sources of data such as EPA dynamometer data, EPA on-board data, and NCHRP dynamometer data for Tier 1 vehicles only were used. The following points have been considered in the development of MOVES to improve the accuracy of its emission estimates compared to the previous emission models:

- applicability to a wide range of spatial and temporal scales (macroscale, mesoscale, and microscale)
- inclusion of all mobile sources at the levels of resolution needed for various applications either operational-level or network-level, and all pollutants (e.g., HC, CO, NO_x, particulate matter, air toxics, and greenhouse gases)
- ease of updating the model, and
- ability to interface with traffic simulation models

One advantage of MOVES is that it is a modal emission model: it derives emission estimates based on second-by-second vehicle performance characteristics for various driving modes. The modal nature of MOVES's emission rates allows the model to more accurately estimate emissions at analysis scales ranging from those associated

with individual transportation projects to large regional emission inventories. The MOVES model serves as the approved model for developing on-road emission estimates for state implementation plans (SIPs) and regional or project-level transportation conformity analyses (Bai et al., 2009).

To estimate modal emission rates, MOVES uses the vehicle specific power (VSP) approach. VSP is an indicator of the vehicle's engine power. With a few simplifying assumptions like assuming no wind, VSP becomes a function of only acceleration, speed, and link's grade. VSP is a useful metric for estimating vehicle emissions and has been used in many studies. The advantage of this metric is that it combines several physical factors like vehicle speed, acceleration, road grade, and road load parameters such as aerodynamic drag and rolling resistance into a single value (Koupal et al., 2003). The VSP measure has a better correlation with emissions than average vehicle speed, which is used by models like EMFAC and MOBILE. VSP values are grouped into 14 bins, and an emission rate, which is measured through on-board measurements, is associated with each bin. Therefore, in order to use the VSP approach, the VSP value should first be calculated and then the corresponding emission rate can be chosen.

MOVES incorporates input data that include vehicle fleet composition, traffic operations, fuel type, and meteorology parameters and conducts modal-based emissions calculations. Based on the resulting modal-based emission rates, emission inventories or emission factors are then generated for a desired geographic scale (macro, meso, or micro scale) as well as temporal resolution (year, day, and hour) (Bai et al., 2009).

The framework of MOVES is made of four major functions: 1) an activity generator, 2) a source bin generator, 3) an operating mode distribution generator, and 4) an emission calculator. The role of these four functions is as follows:

1. Total activity generator: Basic activity data in MOVES are vehicle population and VMT for base year 1999. This function uses growth factors to adapt the

vehicle population and VMT to a target analysis year and then allocates the data by road type, vehicle class, vehicle age, and time period to nationwide observed and projected data from various sources.

2. Source bin distribution generator: The MOVES model classifies vehicles into different source bins. The bins are defined based on combinations of vehicle class, model year group, vehicle weight, engine size and technology, and fuel type. Then source bin fractions are produced to derive weighted emission rates (i.e., the emission rate associated with each bin is weighted by the percentage of vehicles included in that bin).

3. Operating mode distribution generator: It classifies vehicle operating modes into different bins associated with VSP and speed.

4. Emission calculator: This function incorporates modal emission rates into vehicle activity. Generated emission rates from the source bins are first adjusted by a series of factors accounting for parameters like fuel supply and temperature. Then weighted emission rates obtained from function 2 are matched with activities, and the total emissions for a certain type of vehicle in a certain operating mode are estimated.

VT-Micro

The VT-Micro model was developed using chassis dynamometer data on a number of light-duty vehicles and trucks (Rakha et al., 2004b). It is a microscopic modal emission model that estimates vehicle pollutants on a second-by-second basis using either vehicle engine or vehicle speed/acceleration data. Like any other microscopic emission model, using speed and acceleration levels in the emission estimation model not only allows the model to be utilized in conjunction with Global Positioning System (GPS) data for the field evaluation of environmental impacts of operational-level transportation projects (Rakha et al., 2000a, 2004b) but also to be incorporated with

microscopic traffic simulation software that can provide second-by-second trajectory data (Rakha et al., 2000b). Currently, the model has been incorporated with the INTEGRATION microsimulation software (Rakha et al., 2004b).

Unlike MOBILE and EMFAC, which categorize vehicles into general groups of light-duty gasoline vehicle (LDGV), light-duty truck (LDT), and heavy-duty truck (HDV), VT-Micro has a three-level vehicle classification. The first level categorizes vehicles into three groups of light-duty vehicles, light-duty trucks, and heavy-duty trucks. The second level categorizes vehicles based on fuel type (i.e., whether a vehicle is gasoline-fueled or diesel-fueled). Finally, the third level categorizes vehicles using the statistical Classification and Regression Tree (CART) algorithms to further group them into classes that are similar in their emission characteristics. The CART algorithm is a data-mining technique that searches for important patterns and hidden structures in a complex set of data. Applying the CART algorithm to vehicles of the LDGV group, vehicles are further categorized based on model year, engine size, and mileage. Performing the same test for the LDT group, only one variable, the model year, was found to be important for their further categorization (Rakha et al., 2004b).

Comprehensive Modal Emissions Model (CMEM)

CMEM was developed by researchers at the University of California, Riverside along with researchers from the University of Michigan and the Lawrence Berkeley National Laboratory (Barth et al., 2000). It was developed with the goal to evaluate the environmental impacts of operational-level projects as well as considering the modal emission levels of a vehicle. CMEM is a modal emissions model that can estimate emissions for light-duty vehicles (LDVs). The word "comprehensive" refers to its capability of estimating emissions for a wide variety of LDVs in various conditions (e.g., properly functioning, deteriorated, malfunctioning). Like other emission models, the emission rates of CMEM were developed using the chassis dynamometer testing.

Before CMEM, several different approaches had been used for the development of modal emission models. For example, one approach was to set up a speed/acceleration matrix to characterize vehicle operating mode, which contains emission rates for each cell, and another similar matrix that contains time spent in each driving mode (Barth et al., 2000). Therefore, by multiplying these two matrices, the total emissions could be estimated. Although, setting up such matrices is relatively easy, this method does not account for other factors affecting emissions such as road grade, or use of accessories like air conditioner.

Another modal emission modeling approach used is to create an emission map that is based on engine power and speed. By basing emissions on engine power and speed, the effects of acceleration, road grade, and use of accessories are considered. However, in order to create emission inventories, engine power and speed need to be derived from second-by-second velocity profiles, which can be very time-consuming and expensive. In the previous approaches, the matrices are based on steady-state emissions and do not account for transient operations. Additionally, averaging emission rates within each bin and using extrapolation/interpolation among bins is not very realistic and could generate many errors.

One of the key advantages of CMEM is that it uses a modal emission estimation approach that avoids the associated problems that other non-modal emission estimation approaches have. In CMEM, the entire emission estimation process is broken down into different components corresponding to the physical event associated with vehicle operation and emissions production. Then, each component is modeled as an analytical function of certain parameters of that process. These parameters vary by vehicle type, engine, and emission technology. Most of these parameters, which are characteristics of the vehicle such as fuel used per unit of distance or fuel type, are readily available by the vehicle manufacturer. Other important parameters of vehicle operation and emissions production can be obtained by comprehensive testing pro-

grams like dynamometer tests, which are much less complex than creating emission maps for a wide range of vehicle operating modes.

In this modeling method all vehicle factors that have an impact on emissions are taken into account, and different components model the different processes that are related to emissions. Another benefit of this type of modeling is that the major effort is done in the model-development phase rather than in the application phase. Therefore, data required in the application phase is limited compared to other methods. Furthermore, this modal modeling approach makes it possible for CMEM to be used along with both microscale and macroscale vehicle operation characteristics. For example, if the second-by-second velocity profile is available, the model can provide microscopic emission estimates, and if the average speed is available, the physical model can be used based on average power requirements (Barth et al., 2000).

2.1.2 Field Measurements

Field measurements of tailpipe emissions can be performed with the use of on-board instrumentation of vehicles. On-board devices allow measurement of emissions at any location in the network and under any weather conditions. Additionally, since field measurements account for all parameters that affect emissions, they provide more reliable estimates. However, they are not always feasible because of the high cost associated with them. In past years the use of such methods was very limited due to the prohibitively high expenses of the emission measurement devices and other associated costs (Frey et al., 2003). In recent years, with the development of affordable portable instruments, this type of measurements has become more popular.

A portable emission measurement device, which has been widely used for field studies in recent years is the On-board Emission Measurement (OEM 2100) unit. The OEM 2100 is a portable device manufactured by Clean Air Technologies International, Inc (Clean Air Technologies International, Inc., 2015). It can be installed easily in

a light-duty vehicle in approximately 15 minutes. The OEM unit measures mass-flow tailpipe gases, such as CO, CO_2, NO_x, HC, and O_2, during real-world vehicle operations. The OEM consists of two five-gas analyzers, an engine diagnostic scanner, an on-board computer, and it can be connected to the vehicle through the On-Board Diagnostic (OBD) link. This link can get engine and vehicle operational data and import them into the OEM's computer. Since each gas analyzer requires a zeroing procedure every 10 minutes, using two gas analyzers allows the unit to collect data continuously as well as to provide two sets of data that can be averaged at the end (Rakha et al., 2004a). The OEM unit is designed to measure both engine data and emissions from any gasoline-fueled vehicle equipped with an OBD link. This makes it possible to understand the relation between instantaneous speed and vehicle emissions. Figures 2.1(a) and 2.1(b) show how an OEM unit should be installed in a vehicle and how it is connected to vehicle's tailpipe.

(a) OEM 2100 unit

(b) Sampling probe that measures tailpipe emissions

Figure 2.1: OEM 2100 unit installed in a vehicle (Source: Rouphail et al., (2001))

A number of studies have used the OEM unit to estimate emission rates or evaluate the effects of traffic conditions on emissions. Frey et al. (2001a) used the OEM unit to estimate emission rates for different vehicle operation modes. Rouphail et al. (2001) studied the impacts of traffic conditions on real-world vehicle emissions utilizing the OEM unit. Emission rates during each operating mode were measured, and it was demonstrated that the emission rates during acceleration are much higher than other operating modes. In another study by Unal et al. (2003) the impacts of signal coordination strategy on vehicle emissions were evaluated through performing field measurements using OEM-2100. A signal timing plan obtained from SYNCHRO was implemented at two signalized arterials in North Carolina, and changes of HC, NO, and CO emissions, as well as other performance measures were measured. The study showed that signal coordination reduces emissions by 10% to 20% in most cases.

Zhang et al. (2009) also used the OEM unit to measure emission rates required for an integration of the Vehicle Specific Power (VSP) approach with the VISSIM traffic microsimulation software. They evaluated the effects of signal coordination on emissions, and showed a reduction of 50% and 30% for the HC and CO emission factors, respectively, and an increase of 10% for the NO_x emission factor after implementing a coordinated signal timing plan.

A study by Wang et al. (2008) was performed to evaluate the effects of a proposed signal coordination strategy on both emissions and delay using field measurements obtained with OEM-2100. The tested signal coordination strategy resulted in 39.19 kg/hr reduction in total exhaust emissions.

Recently, Salamati et al. (2015) used an OEM unit to measure emission rates needed for the VSP approach in order to compare the emissions produced at signalized intersections and roundabouts. Their study showed that for low demand to capacity ratio, signalized intersections generally produce higher emissions than roundabouts. However, as demand approaches capacity, the emission rates are higher

at roundabouts than signalized intersections. In addition, at oversaturated traffic conditions roundabouts have a steady increase in emissions generated, but signalized intersections show a large jump in the amount of emissions produced as demand exceeds capacity.

2.1.3 Simulation Studies

The majority of studies for evaluating the environmental impacts of traffic management such as signal control strategies have been performed in a simulation environment by integrating an emission model with a traffic microsimulation model such as VISSIM, PARAMICS, CORSIM, INTEGRATION, and AIMSUN (Ahn et al., 2002, Stathopoulos and Noland, 2003, Kun and Lei, 2007, Stevanovic et al., 2009, Chamberlin et al., 2011, Guo and Zhang, 2014, Li et al., 2015) or macrosimulation model such as AVENUE. However, not all studies have used emission rates from existing emission models. Instead, some studies have estimated emission rates through field measurements to use them along with emission calculation approaches (e.g., VSP) (Zhang et al., 2009, Chen et al., 2015).

An integration of MOVES and CMEM with the traffic microsimulation software PARAMICS, was used in a study to evaluate the emission levels resulting from changing a signalized intersection to a roundabout. It was shown that the emissions associated with the roundabout are higher than the signalized intersection for both light and heavy traffic volumes (Chamberlin et al., 2011). Furthermore, Zegeye et al. (2009) integrated the microscopic dynamic emission model, VT-micro, with a microscopic traffic flow model, METANET, to estimate and reduce emissions (CO emission), fuel consumption, and travel time implementing a dynamic speed limit control strategy. They showed that the focus on the reduction of total CO emissions or fuel consumption alone can have negative impacts on the traffic flow under congested traffic conditions. However, when all three measures (i.e., CO emission,

fuel consumption, and travel time) were included in the objective function, the proposed dynamic speed limit control strategy indicated a 40.57%, 23.05%, and 28.26% reduction in total travel time, CO emissions, and fuel consumption, respectively.

In addition to the above studies, some other studies evaluated the impacts of signal control strategies on emissions with the use of simulation software. Guo and Zhang (2014) developed a microsimulation environment by integrating VISSIM and MOVES to define the relationship between mobility and emissions at a signalized intersection controlled by an actuated signal timing plan obtained from SYNCHRO. VSP is one of the most important parameters used in MOVES. The traffic microsimulation tools are used in such studies to find the VSP distribution of vehicles. There are other studies that used VISSIM as the microsimulation tool but this time integrated it with the CMEM emission model to evaluate new signal control strategies in terms of emissions and/or fuel consumption (Stathopoulos and Noland, 2003, Kun and Lei, 2007, Stevanovic et al., 2009). Stathopoulos and Noland (2003) evaluated the effects of traffic flow improvement strategies including signal coordination on both short-term and long-term emissions and fuel consumption. They showed that in most cases long-term emission reductions are unlikely to be achieved. Kun and Lei (2007) evaluated the impacts of 5% increase in the green time of the major direction at a signalized intersection and showed that it can reduce NO_x, CO, and HC emissions produced by cars by 2.6%, 7.2%, and 4.5%, respectively.

Stevanovic et al. (2009) used the VISGAOST signal timing optimization tool and optimized signal timings for different objective functions including minimization of CO_2 emissions and fuel consumption. Although they achieved lower emission and fuel consumption levels when both CO_2 and fuel consumption were included in the objective function at the same time, these objective functions were not always reliable for the optimization of signal timings since they could increase delay significantly. Therefore, they needed to be combined with other traffic performance measures like

vehicle delay. This study also concluded that the lengthy computation times make the application of this research impractical for real-time optimization of signal timings.

Li et al. (2015) utilized a combination of MOVElite (Koupal et al., 2003) and VISSIM. MOVElite is a simplified version of MOVES designed by the U.S. EPA. It considers a limited number of vehicle types. Therefore, it requires fewer emission source bins, a less complex emission rate search process, and is computationally more efficient. In this study, estimates provided in the integrated simulation environment were used along with a Lagrangian Relaxation approach to optimize signal timings by reducing emissions and fuel consumption. The proposed signal control strategy resulted in a 2% reduction in fuel consumption compared to delay-based optimal signal timings when it was implemented for a signalized corridor.

An integration of CORSIM and VT-Micro was used by Park et al., (2009) to estimate emissions and fuel consumption with the goal of developing a sustainable signal control system by minimizing emissions through introducing a speed management strategy. Their system reduced emissions and fuel consumption with moderate trade-offs in delay and stops compared to traditional traffic control strategies, which are aimed at minimizing delay and stops.

Oda et al.(2004) utilized macroscopic estimates of traffic conditions obtained through a macroscopic simulation model, AVENUE, along with regression models to estimate CO_2 in order to investigate the correlation between emissions and both delay and number of stops at arterial roads. They also optimized signal timings by minimizing CO_2 emissions using a meta-heuristic method, and achieved a reduction in CO_2 emissions of 7%.

The INTEGRATION traffic microsimulation tool has also been used along with emission regression models for the purpose of estimating emissions (Rakha et al., 2000a,b). Rakha et al. (2000a) evaluated the impacts of three types of signal coordination (poor, real-time, and good coordination) on delay and emissions, and achieved

significant reductions in emissions (∼50%). It must be noted here that these results are specific to the network and traffic characteristics that were modeled. Specifically, only through-traffic in a single direction was modeled. If cross-street demands were considered in addition to traffic in either direction along the major arterial, the benefits would be less significant.

Although several simulation studies that estimate and minimize emissions at signalized intersections or corridors have been performed, they are not always applicable in the real-world due to their lengthy computation times. Use of microsimulation is also time-consuming and not easily transferable to other sites, since the models need to be re-calibrated and validated for each new test site. Therefore, developing analytical emission estimation model and signal timing optimization strategies that utilize those models while maintaining reasonable computation times for real-time applications is necessary.

2.1.4 Analytical Models

Analytical models have been developed in response to the time-consuming calibrating efforts required for simulation studies and the high cost of field measurements. In addition, they can be applied easier, do not require a lot of parameters to be calibrated, and can provide reliable estimates of emission inventories. Analytical models that are capable of providing accurate emission estimates, are among the most practical approaches and can be incorporated within the existing signal timing process. In recent years, researchers have developed several analytical models to estimate vehicular emissions. These models use average travel characteristics such as speed, delay, and number of stops as inputs (Hellinga et al., 2000).

The 2nd edition of the Canadian Capacity Guide (CCG) presents an emission model, which provides estimates for CO, HC, and NO_x emissions as a function of the number of stops and average stopped delay in each lane during each phase, as

well as the average cruising speed and distance. Therefore, the CCG emission model provides emission estimates as an indirect function of signal timing parameters since the number of stops and average stopped delay are calculated from the traffic demand and signal control parameters (Teply et al., 1995). Hellinga et al. (2000) has also proposed regression models to estimate emissions using traffic demand, roadway characteristics, and traffic signal timing parameters like signal cycle or green splits as explanatory variables.

A number of studies have developed analytical models to first predict vehicle activity (i.e. time spent in each operating mode) at signalized intersections, then use corresponding emission rates for each mode to calculate the total emissions produced (Skabardonis et al., 2013, Shabihkhani and Gonzales, 2013). A key factor in estimating time spent in each mode in these studies is the total number of vehicle stops at the intersection, which is a function of vehicle arrival flow and signal timings. Estimating the number of stops is important because it is directly associated with the number of deceleration/acceleration events that occur before and after each stop, and consequently, the total time spent on these modes. Estimating the number of stops and time spent in different operation modes is usually based on queuing theory (Rakha et al., 2001) or kinematic wave theory (Lighthill and Whitham, 1955; Richards, 1956). Shabihkhani and Gonzales (2013) evaluated the effect of the number of stops and time spent in each operating mode on emissions. They use MOVES to calculate emission rates. They performed the tests for different traffic saturation rates and showed that as traffic conditions approaches saturated conditions, the number of stops increases and consequently, the emissions rates increase significantly.

Skabardonis et al., (2013) evaluated the impacts of optimized signal timings obtained from TRANSYT-7F on delay and emissions. They tested three different objective functions: 1) minimization of system delay, 2) Minimization of system delay and stops with weighting factors for one of the directions, and 3) minimization of

system delay and stops with queue penalty. They showed that minimization of delay and stops either with weighting factor or queue penalty is more effective in reducing emissions because it results in fewer stops and leads to smoother traffic operations. Emission estimates provided in this study were only for autos and transit vehicles were not considered despite of their significant impact on emissions.

2.2 Summary of the Literature

A number of macroscopic and microscopic models have been developed for emission estimation. These models can be incorporated with traffic simulation models to estimate the emissions based on aggregate or second-by-second traffic characteristics. Furthermore, multiple emission estimation studies at signalized intersections have been performed to assess the impact of traffic management strategies on emissions. These studies can be categorized in three groups: 1) field measurements, 2) simulations studies, and 3) analytical studies. Field measurements are not always feasible due to their prohibitively high costs. In addition, they cannot be used for the pre-evaluation of traffic projects. Estimating emissions through simulation software requires a lot of effort since the simulation model needs to be re-calibrated for many parameters for each case. Furthermore, they have long computation times, which makes them inapplicable for real-world uses.

A few studies have developed analytical models to estimate emissions at signalized intersections. However, not all of them have considered the emissions of both autos and transit vehicles. Furthermore, very fewer of these studies have developed signal control strategies to minimize emissions using analytical models. Instead, they use signal timing optimization software such as TRANSYT-7F or SYNCHRO to obtain optimal signal timings.

CHAPTER 3

RESEARCH APPROACH

This chapter presents the goals of this study and the approach used to reach these goals.

3.1 Research Objectives

The objective of this study is twofold: 1) develop an analytical model to estimate emissions for both autos and transit vehicles at isolated intersections that operate at undersaturated traffic conditions, 2) based on this analytical model, develop a real-time signal control system to minimize emissions.

First, the methodology to estimate and minimize emissions is presented. Then, time spent in each vehicle's operating mode is estimated for both autos and transit vehicles. Then, the mathematical program formulation used for calculating the optimal signal timings is developed. Finally, the approach used for modal emission rate estimation is presented and the rates for different vehicle's operating modes for gasoline cars and diesel buses are calculated.

3.2 Research Methodology

The mathematical formulation for the estimation of delay for autos and transit vehicles is based on research by Christofa et al. (2013). Christofa et al. (2013) developed a person-based signal control system that provides priority to transit vehicles by accounting for their higher passenger occupancy. In this thesis the proposed signal control system has utilized the same formulation to estimate time spent in idling

mode for both autos and transit vehicles. After estimating the time spent in idling, a methodology developed by Shabihkhani and Gonzales, (2013) has been utilized to estimate the time spent in acceleration, deceleration, and cruising for both autos and transit vehicles.

The estimated times per operating modes are then multiplied by the corresponding average emission rate of that mode. Accounting for the emissions of different modes separately is necessary, since vehicle emissions vary significantly during different operating modes. The amount of emissions per second spent in acceleration is much higher than other modes. Emission rates are calculated using the Vehicle Specific Power (VSP) approach. Emission rates associated with each VSP bin provided by Zhai et al. (2008) and Frey et al. (2006) for diesel buses and gasoline cars, respectively were utilized.

Several assumptions on driving characteristics, signal control parameters, and traffic conditions are made in order to be able to calculate vehicle operating times, including:

- constant cruising speed and acceleration/deceleration rates;
- constant signal cycle length, phase sequence, and yellow times;
- deterministic vehicle arrival rates;
- fixed and known capacity for each approach; and
- mixed use lanes for autos and transit vehicles.

After developing the model to estimate emissions per operating mode, signal timings are optimized with the goal of minimizing emissions. To account for the effects of signal timing optimization of design cycle T on the next cycle, $T + 1$, the sum of emissions for both cycles are minimized for both autos and transit vehicles as it was

done in the study by Christofa et al. (2013) for total person delay. The optimization program calculates optimal phase splits for every cycle assuming certain upper and lower bounds for the green times of each phase, which guarantee that phases are not skipped and traffic conditions remain undersaturated. The emissions and person delay resulted from the proposed emission-based signal control system are compared with the corresponding outcomes obtained from person-based signal control system developed by Christofa et al. (2013) and the commonly used vehicle-based optimization and the percent changes in both emissions and person delay are reported in chapter 4.

The next section presents the models for estimating time spent in each operating mode first for autos and then for transit vehicles.

3.2.1 Estimating Time Spent in Each Mode

In order to estimate total emissions, we need to account for each vehicle operating mode separately, since emission rates during different modes are considerably different. Therefore, first, the time spent in each mode was estimated and then those times were multiplied by the corresponding emission rate of that mode.

Figure 3.1 illustrates a queuing diagram at an intersection at undersaturated traffic conditions. It can be used to estimate the number of stops as well as the time spent in idling for both autos and transit vehicles. As shown in this figure, each lane group[1] j is assumed to have a constant vehicle arrival rate, which is denoted by q_j.

[1]A lane group is defined as one or more adjacent lanes at each intersection approach that can be served by the same phases (HCM, 2000).

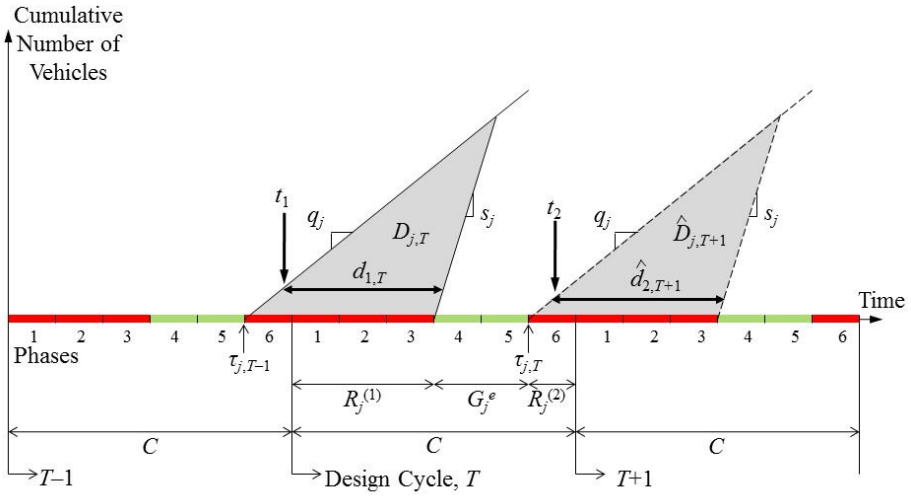

Figure 3.1: Queuing diagram for lane group j for undersaturated conditions, (Source: Christofa et al. (2013))

Certain components of each cycle are defined as follows to simplify the formulation of the analytical model:

$$R_j^{(1)}\left(g_{i,T}\right) = \sum_{i=1}^{k_j-1} g_{i,T} + \sum_{i=1}^{k_j-1} y_i \tag{3.1}$$

$$G_j^e\left(g_{i,T}\right) = \sum_{i=k_j}^{l_j} g_{i,T} + \sum_{i=k_j}^{l_j-1} y_i \tag{3.2}$$

$$R_j^{(2)}\left(g_{i,T}\right) = \sum_{i=l_j+1}^{I} g_{i,T} + \sum_{i=l_j}^{I} y_i \tag{3.3}$$

The generalized formulation of the mathematical program that minimizes emissions for all vehicles at one intersection for a signal cycle T is as follows:

$$min \sum_{a=1}^{A_T} \sum_{m} e_m^a t_{a,m} + \sum_{b=1}^{B_T} \sum_{m} e_m^b t_{b,m} \qquad \forall m \in \{id, cr, acc, dec\} \tag{3.4}$$

$$g_{i\ min} \leq g_{i,T} \leq g_{i\ max} \qquad \forall i \tag{3.5}$$

$$\sum_{i=k_j}^{l_j} g_{i,T} + \sum_{i=k_j}^{l_j-1} y_i \geq g_{j\ min} \qquad \forall j \tag{3.6}$$

$$\sum_{i=1}^{I} g_{i,T} + L = C \tag{3.7}$$

where:

A_T: total number of autos that are considered in the optimization of cycle T;

B_T: total number of transit vehicles that are considered in the optimization of cycle T;

e_m^a: emission rate of autos during operating mode m [gr/sec];

e_m^b: emission rate of transit vehicles during operating mode m [gr/sec];

$t_{a,m}$: time spent in mode m by auto a [seconds];

$t_{b,m}$: time spent in mode m by transit vehicle b [seconds];

id: idling mode;

cr: cruising mode;

acc: acceleration mode;

dec: deceleration mode;

$g_{i,T}$: green time allocated to phase i in cycle T [seconds];

$g_{i\ min/max}$: minimum/maximum green time of phase i [seconds];

k_j/l_j: first/last phase in a cycle that can serve lane group j;

y_i: yellow time for phase i [seconds];

$g_{j/min}$: minimum green time of lane group j [seconds];

I: total number of phases in a cycle;

L: total lost time per cycle [seconds];

C: cycle length [seconds].

The next sections explain the models that are used to estimate time spent in each mode for autos and transit vehicles, separately.

Auto Vehicles

Time Spent Accelerating/Decelerating

To calculate time spent in deceleration/acceleration, we first estimated the number of stops because before and after each stop, vehicles spend some time in these modes. At undersaturated conditions, which is the focus of this thesis, vehicles stop at most once upstream of the intersection so, the total number of vehicle stops is equal to the number of vehicles in queue. As mentioned before to account for the effects of signal timing optimization of the design cycle T on the next cycle, $T+1$, the sum of auto emissions for both cycles is included in the objective function. Considering Figure 3.1, the number of stops can be calculated by equations 3.8 and 3.9. These equations, which have been adopted by Shabihkhani and Gonzales (2013) calculate auto vehicle stops for cycles T, $N_{s,T}$ and $T+1$, $N_{s,T+1}$.

$$N_{s,T} = \sum_{j=1}^{J} \frac{q_j}{1-\frac{q_j}{s_j}} \left(R_j^{(2)}(g_{i,T-1}) + R_j^{(1)}(g_{i,T}) \right) \tag{3.8}$$

$$N_{s,T+1} = \sum_{j=1}^{J} \frac{q_j}{1-\frac{q_j}{s_j}} \left(R_j^{(2)}\left(g_{i,T}\right) + R_j^{(1)}\left(g_{i\ next}\right) \right) \tag{3.9}$$

where q_j and s_j measured in [vph] are the auto arrival flow and the saturation flow of lane group j, respectively. J is the number of lane groups at the intersection, and $g_{i\ next}$ is the green time for phase i for cycle $T+1$, which for the purpose of this study was set to the provided fixed optimal green times by TRANSYT-7F (Wallace et al., 1984). The assumed values for $g_{i\ next}$ do not affect the results considerably since they will be updated in the optimization of cycle $T+1$.

To estimate acceleration/deceleration times from a stop to cruising speed or vice versa first the cruising speed is divided by the constant acceleration/deceleration rate.

This gives the acceleration/deceleration time for each stop. These calculated times are multiplied by the number of stops to provide an estimation for the whole time spent in these modes during a cycle. The total time spent in acceleration/deceleration modes during cycles T, $t_{acc/dec,T}$, and $T+1$, $t_{acc/dec,T+1}$, can be estimated by equations 3.10 and 3.11.

$$t_{a,acc/dec,T} = \frac{v_{a,cr}}{a_{a,acc/dec}} \left[\sum_{j=1}^{J} \frac{q_j}{1 - \frac{q_j}{s_j}} \left(R_j^{(2)}(g_{i,T-1}) + R_j^{(1)}(g_{i,T}) \right) \right] \tag{3.10}$$

$$t_{a,acc/dec,T+1} = \frac{v_{a,cr}}{a_{a,acc/dec}} \left[\sum_{j=1}^{J} \frac{q_j}{1 - \frac{q_j}{s_j}} \left(R_j^{(2)}(g_{i,T}) + R_j^{(1)}(g_{i\ next}) \right) \right] \tag{3.11}$$

where $v_{a,cr}$ is the average cruising speed of approaching autos in [m/s], and $\alpha_{a,acc/dec}$ is the average acceleration/deceleration rate of autos in $[m/s^2]$.

Time Spent Idling

Figure 3.2 shows the trajectories of vehicles as they travel from a distance upstream the intersection and pass the intersection. As shown in this figure, vehicles that have to stop first travel at cruising speed, then arrive at the intersection and stop at the back of the queue, and then when the signal turns green, they move forward at cruising speed. Note that the time-space diagram is drawn assuming that traffic conditions can be represented by a triangular fundamental diagram as the one shown in Figure 3.3. However, in reality vehicles cannot instantaneously stop or reach cruising speed, but they travel some time in acceleration/deceleration mode as shown in Figure 3.4. As Figure 3.4 indicates that some of the time we consider as idling or cruising is actually spent on deceleration and acceleration. Therefore, half of the required time for acceleration and deceleration is subtracted from the idling mode and half of it is subtracted from the cruising mode.

Queuing diagrams such as the one illustrated in Figure 3.1 allow us to estimate delays (i.e., idling time) for both autos and transit vehicles. Since the y-axis of

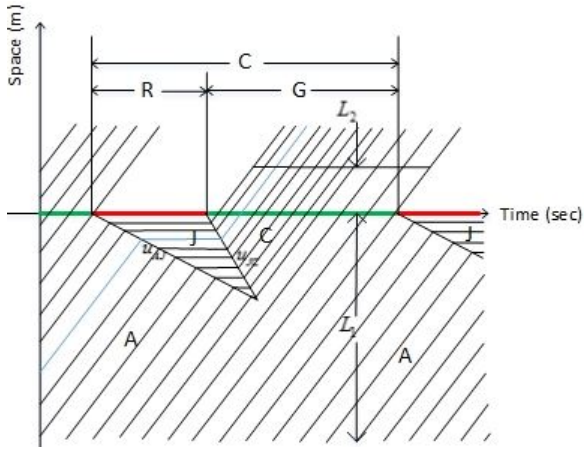

Figure 3.2: Time-space diagram for an intersection approach in undersaturated conditions

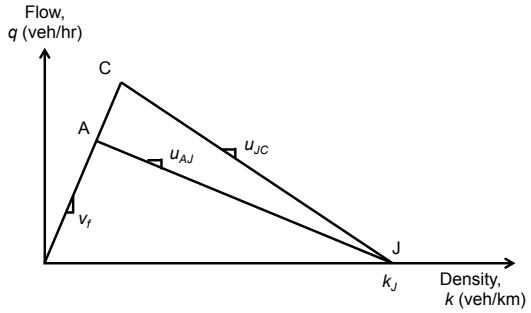

Figure 3.3: Fundamental diagram

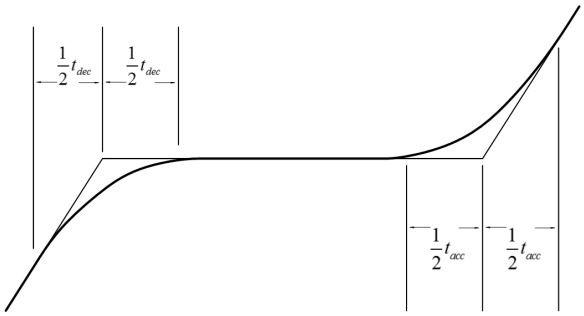

Figure 3.4: Acceleration-deceleration cycle for a single stop

this graph represents the cumulative number of vehicles the areas $D_{j,T}$ and $\hat{D}_{j,T+1}$ represent the total auto delay at the intersection for cycles T and $T+1$, respectively. However, half of the total acceleration and deceleration time should be subtracted

from the total auto delay for cycle T, $D_{j,T}$, and the total auto delay for cycle $T+1$, $\hat{D}_{j,T+1}$. Therefore, for all autos that stop, the total time spent idling in cycles T, $t_{a,id,T}$, and $T+1$, $t_{a,id,T+1}$, can be calculated as follows:

$$t_{a,id,T} = \frac{1}{2}\sum_{j=1}^{J}\left[\frac{q_j}{1-\frac{q_j}{s_j}}\Big(R_j^{(2)}(g_{i,T-1}) + R_j^{(1)}(g_{i,T})\Big)^2 - \Big(\frac{t_{a,acc,T}+t_{a,dec,T}}{2}\Big)\right] \tag{3.12}$$

$$t_{a,id,T+1} = \frac{1}{2}\sum_{j=1}^{J}\left[\frac{q_j}{1-\frac{q_j}{s_j}}\Big(R_j^{(2)}(g_{i,T}) + R_j^{(1)}(g_{i\ next})\Big)^2 - N_{s,T+1}\Big(\frac{t_{a,acc,T+1}+t_{a,dec,T+1}}{2}\Big)\right] \tag{3.13}$$

Time Spent Cruising

The last operating mode whose duration needs to be estimated is the cruising mode. For the estimation of cruising time we need to consider certain lengths for sections both upstream and downstream of the intersection to ensure that stopping vehicles experience a full operation cycle (i.e., cruising, deceleration, idling, acceleration, and cruising again). This adjustment is made because not all vehicles experience a full operation cycle. These two distances are defined as L_1 and L_2 and are shown in Figure 3.2. L_1 and L_2 should be long enough that any vehicle experiences a complete operation cycle. The cruising time of vehicles during cycles T and $T+1$ are estimated by equations 3.14 - 3.19. Equations 3.14 and 3.17 calculate time spent in cruising mode for vehicles that have to stop in cycles T and $T+1$, which are denoted by $t_{a,cr,T}^{(1)}$ and $t_{a,cr,T+1}^{(1)}$, respectively. Autos that arrive during the green phase after the clearance of their lane group's queue can pass the intersection without stopping and travel the whole link distance in cruising mode. Equations 3.15 and 3.18 calculate time spent in cruising mode for vehicles that do not have to stop in cycles T and $T+1$, which are denoted by $t_{a,cr,T}^{(2)}$ and $t_{a,cr,T+1}^{(2)}$, respectively. Then, the total time spent in cruising mode in each cycle, $t_{a,cr,T}$ and $t_{a,cr,T+1}$, is calculated by Equations 3.16 and 3.19.

$$t^{(1)}_{a,cr,T} = \left[\frac{q_j}{1-\frac{q_j}{s_j}}\Big(R^{(2)}_j(g_{i,T-1}) + R^{(1)}_j(g_{i,T})\Big)\Big(\frac{L_1+L_2}{v_{a,cr}}\Big)\right] - \frac{1}{2}(t_{a,acc,T} + t_{a,dec,T}) \quad (3.14)$$

$$t^{(2)}_{a,cr,T} = \frac{L_1+L_2}{v_{a,cr}}\left[q_j C - \frac{q_j}{1-\frac{q_j}{s_j}}\left(R^{(2)}_j(g_{i,T-1}) + R^{(1)}_j(g_{i,T})\right)\right] \quad (3.15)$$

$$t_{a,cr,T} = t^{(1)}_{a,cr,T} + t^{(2)}_{a,cr,T} \quad (3.16)$$

$$t^{(1)}_{a,cr,T+1} = \left[\frac{q_j}{1-\frac{q_j}{s_j}}\Big(R^{(2)}_j(g_{i,T}) + R^{(1)}_j(g_{i\ next})\Big)\Big(\frac{L_1+L_2}{v_{a,cr}}\Big)\right] - \frac{1}{2}(t_{a,acc,T+1} + t_{a,dec,T+1}) \quad (3.17)$$

$$t^{(2)}_{a,cr,T+1} = \frac{L_1+L_2}{v_{a,cr}}\left[q_j C - \frac{q_j}{1-\frac{q_j}{s_j}}\Big[R^{(2)}_j(g_{i,T}) + R^{(1)}_j(g_{i\ next})\Big]\right] \quad (3.18)$$

$$t_{a,cr,T+1} = t^{(1)}_{a,cr,T+1} + t^{(2)}_{a,cr,T+1} \quad (3.19)$$

where C is the cycle length [seconds]. Therefore, the total auto emission component of the objective function is as follows:

$$\sum_{a=1}^{A_T}\sum_m e^a_m t_{a,m} + \sum_{a=1}^{A_{T+1}}\sum_m e^a_m t_{a,m} = e^a_{id}t_{a,id,T} + e^a_{cr}t_{a,cr,T} + e^a_{acc}t_{a,acc,T} + e^a_{dec}t_{a,dec,T} + e^a_{id}t_{a,id,T+1} + e^a_{cr}t_{a,cr,T+1} + e^a_{acc}t_{a,acc,T+1} + e^a_{dec}t_{a,dec,T+1} \quad (3.20)$$

Transit Vehicles

The time estimation for all operating modes of transit vehicles is similar to auto vehicles except for the idling mode. For estimation of transit delay we only consider transit vehicles that are served or arrive during design cycle T. Transit vehicles that arrive in cycle $T+1$ are not taken into account for the optimization of cycle T since their arrival time information is not available when optimizing cycle T. Transit vehicles that arrive during cycle $T+1$ are considered in the optimization of the next cycle.

Assuming that transit vehicles decelerate or accelerate at a constant rate, the total time spent on these modes during cycle T, $t_{b,acc/dec,T}$, can be estimated as follows:

$$t_{b,acc/dec,T} = \frac{v_{b,cr}}{a_{b,acc/dec}} \tag{3.21}$$

where $v_{b,cr}$ is the cruising speed for transit vehicle b in [m/sec], and $a_{b,acc/dec}$ is the average acceleration/deceleration rate of transit vehicle b in [m/sec^2].

The idling time (i.e., delay) of a bus, b, depends on its arrival time, t_b, relative to the end of the last phase that can serve its lane group in cycles $T-1$ and T, which are denoted by $\tau_{j,T-1}$ and $\tau_{j,T}$, respectively (see Figure 3.1) and can be expressed as follows:

$$\tau_{j,T-1} = (T-2)\,C + R_j^{(1)}\left(g_{i,T-1}\right) + G_j^e\left(g_{i,T-1}\right) \tag{3.22}$$

$$\tau_{j,T} = (T-1)\,C + R_j^{(1)}\left(g_{i,T}\right) + G_j^e\left(g_{i,T}\right) \tag{3.23}$$

Figure 3.1 also shows examples of two transit vehicles that arrive at times t_1 and t_2 and their corresponding delays, $d_{1,T}$ and $\hat{d}_{2,T+1}$ that are used to estimate bus idling time. Transit vehicles are categorized into three groups based on their arrival time:

- Transit vehicles that arrive before the end of the green phases that can serve them in cycle T and before the queue has dissipated. This time interval is denoted as α. $d_{1,T}$ in Figure 3.1 represents the idling time for a transit vehicle of this group.

- Transit vehicles that arrive before the end of the green phases that can serve them in cycle T but after the queue has dissipated. The time interval of this group is denoted as β. These vehicles experience no delay and pass through the intersection without stopping.

- Transit vehicles that arrive after the end of their green phase in cycle T. This time interval is denoted as γ. $\hat{d}_{2,T+1}$ represents the delay for a transit vehicle in this group.

The idling time for transit vehicles of the above mentioned groups, accounting for the fact that half of the idling time is allocated to acceleration/deceleration modes, as it was the case for autos, is calculated by equations 3.24 - 3.26.

$$t^{\alpha}_{b,id,T} = (T-1)\,C + R^{(1)}_{j}\left(g_{i,T}\right) + \frac{q_j}{s_j}\left(t_b - \tau_{j,T-1}\right) - t_b - \left(\frac{t_{b,acc,T} + t_{b,dec,T}}{2}\right) \quad (3.24)$$

$$t^{\beta}_{b,id,T} = 0 \quad (3.25)$$

$$t^{\gamma}_{b,id,T} = TC + R^{(1)}_{j}(g_{i\ next}) + \frac{q_j}{s_j}(t_b - \tau_{j,T}) - t_b - \left(\frac{t_{b,acc,T} + t_{b,dec,T}}{2}\right) \quad (3.26)$$

where $t^{\alpha}_{b,id,T}$, $t^{\beta}_{b,id,T}$, and $t^{\gamma}_{b,id,T}$ are the time spent in idling mode by transit vehicles that arrive in time intervals α, β, and γ, respectively.

Therefore, the cruising time of transit vehicles that stop and do not stop during cycle T is given by equations 3.27 and 3.28, respectively:

$$t^{\alpha/\gamma}_{b,cr,T} = \frac{L_1 + L_2}{v_{b,cr}} - \frac{t_{b,acc,T} + t_{b,dec,T}}{2} \quad (3.27)$$

$$t^{\beta}_{b,cr,T} = \frac{L_1 + L_2}{v_{b,cr}} \quad (3.28)$$

In order to consider the right equations for a transit vehicle's operating time, three integer variables, $(\omega^{\alpha}_b, \omega^{\beta}_b, \omega^{\gamma}_b)$, which correspond to time intervals, (α, β, γ), are introduced. If the transit vehicle arrives during interval f, ω^{f}_b will be equal to 1, otherwise it will be 0 for $f \in \{\alpha, \beta, \gamma\}$. Therefore, the transit emission component of the objective function becomes:

$$\sum_{b=1}^{B_T}\Bigg[e_{acc}^{b}\Big[(\omega_b^{\alpha}+\omega_b^{\gamma})t_{b,acc,T}\Big]+e_{dec}^{b}\Big[(\omega_b^{\alpha}+\omega_b^{\gamma})t_{b,dec,T}\Big]$$
$$+e_{id}^{b}\Big[\omega_b^{\alpha}\big[(T-1)C+R_j^{(1)}(g_{i,T})+\frac{q_j}{s_j}(t_b-\tau_{j,T-1})-t_b-\big(\frac{t_{b,acc,T}+t_{b,dec,T}}{2}\big)\big]\Big]$$
$$+\omega_b^{\gamma}\big[TC+R_j^{(1)}(g_{i\ next})+\frac{q_j}{s_j}(t_b-\tau_{j,T})-t_b-\big(\frac{t_{b,acc,T}+t_{b,dec,T}}{2}\big)\big]\Big]$$
$$+e_{cr}^{b}\Bigg[(\omega_b^{\alpha}+\omega_b^{\gamma})\Big[\Big(\frac{L_1+L_2}{v_{b,cr}}\Big)-\Big(\frac{t_{b,acc,T}+t_{b,dec,T}}{2}\Big)\Big]+\omega_b^{\beta}\Big(\frac{L_1+L_2}{v_{b,cr}}\Big)\Big]\Bigg] \quad (3.29)$$

The constraints of person delay component for transit vehicles are as follows:

$$(T-1)C+R_j^{(1)}g(i,T)+\frac{q_j}{s_j}(t_b-\tau_{j,T-1})-t_b\geq-(1-\omega_b^{\alpha})M_1 \quad \forall b \quad (3.30)$$

$$(T-1)C+R_j^{(1)}g(i,T)+\frac{q_j}{s_j}(t_b-\tau_{j,T-1})-t_b\leq\omega_b^{\alpha}M_1 \quad \forall b \quad (3.31)$$

$$(1-\omega_b^{\gamma})t_b\leq\tau_{j,T} \quad \forall b \quad (3.32)$$

$$(1-\omega_b^{\gamma})M_2+\omega_b^{\gamma}t_b\geq\tau_{j,T} \quad \forall b \quad (3.33)$$

$$G_j^{e}(g_{i,T})\geq\frac{q_j}{s_j}C \quad \forall j \quad (3.34)$$

$$\sum_{i=1}^{I}g_{i,T}+\sum_{i=1}^{I}y_i=C \quad (3.35)$$

$$g_{i,T}\geq g_{i/min} \quad \forall i \quad (3.36)$$

$$g_{i,T}\leq g_{i/max} \quad \forall i \quad (3.37)$$

$$\omega_b^{\alpha}+\omega_b^{\beta}+\omega_b^{\gamma}=1 \quad \forall b \quad (3.38)$$

$$\omega_b^{\alpha},\ \omega_b^{\beta},\ \omega_b^{\gamma} \in \{0,1\} \qquad \forall b \tag{3.39}$$

where M_1 and M_2 are big numbers. Constraints 3.30 to 3.33 ensure that the correct delay formula is used for each transit vehicle. Constraint 3.34 ensures undersaturated traffic conditions for each lane group. Constraint 3.35 ensures the sum of obtained green times and fixed lost time equals to the cycle length. Constraints 3.36 and 3.37 set lower and upper bounds for green times. Finally, constraints 3.38 and 3.39 ensure that only one binary variable equals to one (Christofa et al., 2013).

3.2.2 Mathematical Program Formulation

The optimization problem in this study has a quadratic objective function and linear constraints. The existence of quadratic terms in addition to the multiplication of $g_{i,T}$, which are continuous variables with ω^f, which are integer variables leads to biliniarities. Hence, this mathematical program is a Mixed Integer Non-Linear Program (MINLP). To deal with this problem the method suggested by Floudas (1995) and used by Christofa et al., (2013) has also been used in this thesis. Three new continuous variables, $g_{i,b}^{\alpha}$, $g_{i,b}^{\beta}$, and $g_{i,b}^{\gamma}$, corresponding to α, β, and γ are introduced for each transit vehicle b such that:

$$g_{i,T} = g_{i,b}^{\alpha} + g_{i,b}^{\beta} + g_{i,b}^{\gamma} \qquad \forall i, b \tag{3.40}$$

where:

$$g_{i,b}^{\beta} = g_{i,b}^{\gamma} = 0 \qquad \forall i, b\ if t_b \in \alpha \tag{3.41}$$

$$g_{i,b}^{\alpha} = g_{i,b}^{\gamma} = 0 \qquad \forall i, b\ if t_b \in \beta \tag{3.42}$$

$$g_{i,b}^{\alpha} = g_{i,b}^{\beta} = 0 \qquad \forall i, b\ if t_b \in \gamma \tag{3.43}$$

The transit emission component of the objective function based on new green time variables becomes as shown in 3.44.

$$\sum_{b=1}^{B_T}\Bigg[e^b_{acc}\Big[(\omega^\alpha_b+\omega^\gamma_b)t_{b,acc,T}\Big]+e^b_{dec}\Big[(\omega^\alpha_b+\omega^\gamma_b)t_{b,dec,T}\Big]$$
$$+e^b_{id}\Bigg[\omega^\alpha_b\Big[(T-1)C+\sum_{i=1}^{k_j-1}y_i+\frac{q_j}{s_j}(t_b-\tau_{j,T-1})-t_b-\Big(\frac{t_{b,acc,T}+t_{b,dec,T}}{2}\Big)\Big]$$
$$+\omega^\gamma_b\Big[TC+R^{(1)}_j(g_{i\ next})+\frac{q_j}{s_j}\Big(t_b-(T-1)C-\sum_{i=1}^{l_j-1}y_i\Big)-t_b-\Big(\frac{t_{b,acc,T}+t_{b,dec,T}}{2}\Big)\Big]\Bigg]$$
$$+e^b_{cr}\Bigg[(\omega^\alpha_b+\omega^\gamma_b)\Big[\Big(\frac{L_1+L_2}{v_{b,cr}}\Big)-\Big(\frac{t_{b,acc,T}+t_{b,dec,T}}{2}\Big)\Big]+\omega^\beta_b\Big(\frac{L_1+L_2}{v_{b,cr}}\Big)\Big]\Bigg]$$
$$+e^b_{id}\sum_{i=1}^{k_j-1}g^\alpha_{i,b}-e^b_{id}\frac{q_j}{s_j}\sum_{i=1}^{l_j}g^\gamma_{i,b}\Bigg] \quad (3.44)$$

Constraints 3.36 and 3.37 are replaced by

$$g^f_{i,b}\geq\omega^f_b g_{i\ min}\quad\forall i,b\ \ \forall f\in\{\alpha,\beta,\gamma\} \quad (3.45)$$

$$g^f_{i,b}\leq\omega^f_b g_{i\ max}\quad\forall i,b\ \ \forall f\in\{\alpha,\beta,\gamma\} \quad (3.46)$$

The optimization problem in this study is solved with the use of the Branch and Bound method to identify the global minimum as long as the objective function remains convex. For the solution of the subsequent non-linear programs of each branch MATLAB's function fmincon is utilized.

3.2.3 Modal Emission Rates Estimation

Frey et al. (2001b) has performed field measurements to estimate emission rates for different vehicle operating modes: acceleration, deceleration, cruise, and idle. Many studies that calculate vehicle modal emissions use such emission rates assuming constant speed and acceleration rates for the entire time of each mode (Skabardonis et al., 2013). However, these rates are not good representatives of the emissions produced in acceleration and deceleration because of the speed changes that occur during these modes, i.e., calculating the VSP value based on an average speed for the

whole acceleration or deceleration is oversimplifying since there are speed changes from zero to cruising speed and vice versa. Assuming the same speed for whole time the vehicle is operating in these modes could lead to inaccurate emission estimates particularly for pollutants like CO and HC that are very sensitive to speed changes (Rakha and Ding, 2003).

In order to estimate more accurate emissions rates for each mode, first the VSP mode for every second is calculated using the constant acceleration/deceleration rate and the average value of the speed for that time interval. Then, the emission rates for each VSP mode are estimated (for three pollutants, CO, HC, NO_x) based on the rates provided by Zhai et al. (2008) for diesel buses and Frey et al. (2006) for gasoline autos. Finally, in order to calculate emission rates for acceleration, deceleration, idling, and cruising modes separately, the emission rates of the VSP bins included in these modes are averaged.

The assumed free flow speeds and acceleration/deceleration rates for autos and buses that are used to calculate the VSP modes are consistent with the values used in the simulation tests and are as follows:

$v_{f,car} = 45\frac{km}{hr} = 12.5\frac{m}{s}$ $\qquad$ $v_{f,bus} = 45\frac{km}{hr} = 12.5\frac{m}{s}$

$acc_{car} = 3\frac{m}{s^2}$ $\qquad$ $acc_{bus} = 2\frac{m}{s^2}$

$dec_{car} = 4\frac{m}{s^2}$ $\qquad$ $dec_{bus} = 2\frac{m}{s^2}$

The idling autos fall into VSP mode 3. In addition, assuming a value of 45 km/hr for the free flow speed the cruising mode falls under VSP mode 4. Also, the idling buses fall into VSP mode 1. In addition, assuming a value of 45 km/hr for the free flow speed the cruising mode falls under VSP mode 2.

Tables 3.1 to 3.6 show the process of emission rates calculation for both autos and buses.

Table 3.1: Calculation of modal emission rates for gasoline autos for acceleration

Time [*sec*]	Speed [m/s]	Average Speed [m/s]	VSP [kw/ton]	VSP mode	NO_x [mg/s]	HC [mg/s]	CO [mg/s]
$[0-1]$	$[0-3]$	1.5	5.15	5	1.7	0.5	11.0
$[1-2]$	$[3-6]$	4.5	15.47	8	4.2	1.0	29.2
$[2-3]$	$[6-9]$	7.5	25.77	11	7.6	2.1	113.8
$[3-4]$	$[9-12]$	10.5	36.39	13	15.5	4.9	441.8
$[4-4.17]$	[12.12.5]	12.25	42.60	14	17.9	10.9	882.3
Average					7.7	2.5	178.3

Table 3.2: Calculation of modal emission rates for gasoline autos for deceleration

Time [*sec*]	Speed [m/s]	Avg Speed [m/s]	VSP [kw/ton]	VSP mode	NO_x [mg/s]	HC [mg/s]	CO [mg/s]
$[0-1]$	$[12.5-8.5]$	10.5	-44.46	1	0.9	0.5	7.8
$[1-2]$	$[8.5-4.5]$	6.5	-27.66	1	0.9	0.5	7.8
$[2-3]$	$[4.5-0.5]$	2.5	-10.67	1	0.9	0.5	7.8
$[3-3.13]$	$[0.5-0]$	0.25	-1.07	2	0.6	0.3	3.9
Average					0.9	0.5	7.6

Table 3.3: Modal emission rates for gasoline autos

Operating mode	NO_x [mg/s]	HC [mg/s]	CO [mg/s]
Acceleration	7.7	2.5	178.3
Deceleration	0.9	0.5	7.6
Cruising	1.2	0.4	8.3
Idling	0.3	0.4	3.3

Table 3.4: Calculation of modal emission rates for diesel buses for acceleration

Time [*sec*]	Speed [m/s]	Avg Speed [m/s]	VSP [kw/ton]	VSP mode	NO_x [mg/s]	HC [mg/s]	CO [mg/s]
$[0-1]$	$[0-2]$	1.00	2.09	2	133	1.75	35.0
$[1-2]$	$[2-4]$	3.00	6.28	4	220	1.85	73.0
$[2-3]$	$[4-6]$	5.00	10.49	6	255	2.1	95.0
$[3-4]$	$[6-8]$	7.00	14.72	8	320	2.2	60.0
$[4-5]$	$[8-10]$	9.00	18.98	8	320	2.2	60.0
$[5-6]$	$[10-12]$	11.00	23.29	8	320	2.2	60.0
$[6-6.25]$	$[12-12.5]$	12.25	26.01	8	320	2.2	60.0
Average					263.6	2.1	63.6

Table 3.5: Calculation of modal emission rates for diesel buses for deceleration

Time [*sec*]	Speed [m/s]	Avg Speed [m/s]	VSP [kw/ton]	VSP mode	NO_x [mg/s]	HC [mg/s]	CO [mg/s]
$[0-1]$	$[12.5-10.5]$	11.5	-21.62	1	45.0	1.3	8.6
$[1-2]$	$[10.5-8.5]$	9.5	-17.95	1	45.0	1.3	8.6
$[2-3]$	$[8.5-6.5]$	7.5	-14.22	1	45.0	1.3	8.6
$[3-4]$	$[6.5-4.5]$	5.5	-10.45	1	45.0	1.3	8.6
$[4-5]$	$[4.5-2.5]$	3.5	-6.67	1	45.0	1.3	8.6
$[5-6]$	$[2.5-0.5]$	1.5	-2.86	1	45.0	1.3	8.6
$[6-6.25]$	$[0.5-0]$	0.25	-0.48	1	45.0	1.3	8.6
Average					45.0	1.3	8.6

Table 3.6: Modal emission rates for diesel buses

Operating mode	NO_x[mg/s]	HC [mg/s]	CO[mg/s]
Acceleration	263.5	2.1	63.6
Deceleration	45.0	1.3	8.6
Cruising	133.3	1.7	37.1
Idling	45.0	1.3	8.6

CHAPTER 4

EVALUATION

This chapter presents types of tests performed for the evaluation of the proposed emission-based signal control system. Then, two test sites whose traffic data is used in the evaluation tests are described. Finally, the results of these tests are presented.

4.1 Evaluation Tests

The performance of the proposed signal control system is evaluated with the use of two types of tests: 1) deterministic arrival tests and 2) stochastic arrival tests. Deterministic arrival tests are performed under the assumption that perfect information about the transit vehicle arrival times, auto flows and arrival times, as well as auto and transit vehicles' passenger occupancies are available in real time without errors. In addition, the auto vehicle arrival flows at each lane group are assumed to be constant across all cycles. Deterministic arrival tests also assume constant acceleration and deceleration rates. On the other hand, stochastic arrival tests are performed through the microsimulation software AIMSUN (TSS, 2010) using Emulation-In-the-Loop Simulation (EILS). EILS utilizes the Advanced Programming Interface (API) of AIMSUN, to model the proposed traffic signal control system, as well as the previously published person-based signal timing optimization algorithm (Christofa et al., 2013). This way, the real-time signal control system can be tested in a more realistic environment where there is stochasticity in auto arrival flows and times as well as transit vehicle arrival times and transit passenger occupancies.

For stochastic arrival tests, the prediction of auto arrivals is based on two sets of detectors. The first set of detectors are located at a certain distance upstream of the intersection and the other set are located at the exit of each lane group. Exponential smoothing is used the auto arrival flows. The vehicle arrival measurements obtained by these two sets of detectors during the precious cycle are used to predict auto arrival flows as follows

$$\hat{q}_{j,T} = eq_{j,T-1} + (1-e)\hat{q}_{j,T-1} \tag{4.1}$$

where $\hat{q}_{j,T}$ is a weighted average of the prediction $\hat{q}_{j,T-1}$ and the observed value $q_{j,T-1}$ of the previous cycle. A value of $e = 0.2$ is used in this study. The arrival flows used in the optimization of cycle T is the maximum of two smoothed flows of the previous cycle from two sets of detectors. In this way all demand that was not served in the previous cycle are accounted for in the optimization of this cycle (Christofa et al., 2013).

The timetable of the transit vehicle arrivals at the entry links of the network is fixed and based on the same headways as in the deterministic arrival tests. Transit vehicle arrival times are predicted based on information collected by detectors located upstream on entry links at distances from the intersection equivalent to the travel time of one cycle length. This way, a transit vehicle's arrival at the intersection can be known one cycle in advance and therefore, this information can be used for the signal timing optimization of the next cycle. The transit vehicle arrivals at the approaches are predicted using an average nominal speed of 45 km/h.

As mentioned before, $g_{i,next}$ is a user specified value for the green time of the next cycle, which is used to estimate the delay and emissions of the next cycle. It is set to the initial value of the fixed optimized green times obtained by TRANSYT-7F (Wallace et al., 1984) for both types of tests. The green times of each phase are constrained by maximum and minimum green times, g_{imax} and g_{imin}. For both types

of tests g_{imax} is set to $C - \sum_{i=1}^{I} y_i$, and g_{imin} is set to 7 seconds for left-turning movements and to 10 seconds for through movements.

In order to predict person delay an average passenger occupancy of 1.25 passengers/vehicle is used for autos. Also, the average passenger occupancy for each transit vehicle is assigned a random number of passengers with an average value of 40 passengers/vehicle.

The normal acceleration and deceleration rates of auto vehicles at urban intersections are considered to be 3 m/s^2 and 4 m/s^2, respectively. Transit vehicles are assumed to have the same rate for both acceleration and deceleration which is equal to 2 m/s^2. An average cruising speed of 45 km/hr is considered for both auto and transit vehicles for both test sites, which are described in the next section. These inputs are consistent between the two types of tests. Also, each type of tests is performed 20 times to account for variability in auto and bus arrivals.

Both types of tests are performed using the aforementioned inputs for different intersection flow ratios [1] (Y) form $Y = 0.4$ to $Y = 0.9$ for the first intersection and $Y = 0.4$ to $Y = 0.73$ for the second intersection to evaluate the impacts of traffic volume on emissions.

In order to evaluate the performance of the proposed emission-based signal control system, to types of comparison are performed. First type compares the emissions and person delay obtained from emission-based optimization with those obtained from previously developed person-based optimization by Christofa et al. (2013). The other type compares obtained emissions and person delay obtained from emission-based and commonly-used vehicle based optimization.

---

[1]Intersection flow ratio: the sum of flow ratios (the ratio of demand to saturation flow) for each critical lane group per signal phase at the intersection (HCM, 2000).

4.2 Study Sites

The evaluation of the proposed emission-based signal control system is conducted using geometric, traffic, and signal timing data from two real-world intersections: 1) intersection of Mesogion and Katechaki Avenues located in Athens, Greece and 2) intersection of University and San Pablo Avenues, located in Berkeley, CA.

4.2.1 Intersection of Mesogion and Katechaki Avenues

This intersection features high traffic volumes and nine conflicting transit routes with headways that vary from 15 to 40 minutes for each route. Figure 4.1 illustrates the intersection's layout and bus routes that travel through it. The bus routes run in four conflicting directions with 70% traveling in northeast-southwest approaches (Mesogion Avenue) and 30% on the northwest-southeast approaches (Katechaki Avenue). Autos and buses share the same lanes. The intersection also includes bus stops, which however are ignored for the purpose of this study.

The volume data have been obtained by detectors located 40 meters upstream of the intersection for 7:00 AM to 8:00 AM (the morning peak), which is the analysis period. The intersection operates on a six-phase cycle and has a flow ratio of $Y = 0.9$ during the morning peak hour. An intersection flow ratio of 0.9 implies conditions close to saturation, considering a cycle length $C = 120$ seconds and lost time $L = 14$ seconds. Information about the bus schedule will be obtained by the Athens Urban Transport Organization's website (2010).

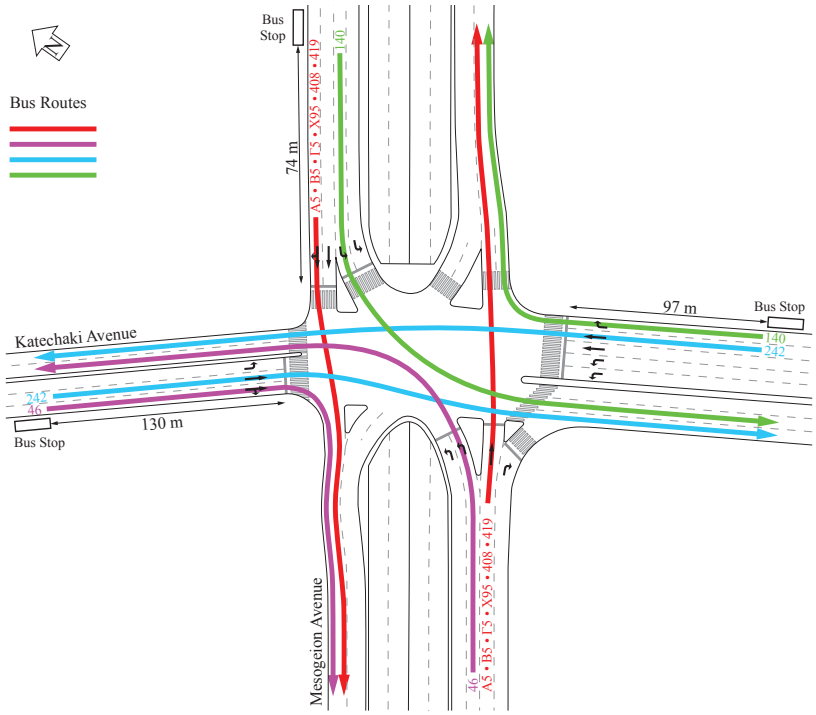

Figure 4.1: Layout and bus routes for the intersection of Mesogion and Katechaki Avenues, (Source: Christofa et al. (2013)).

4.2.2 Intersection of University and San Pablo Avenues

The intersection of University and San Pablo Avenue is also characterized by high traffic volumes and it serves several conflicting bus routes. Figure 4.2 shows the intersection layout and bus routes that travel through it. There are six bus routes passing the intersections, which share the same lanes with other traffic. Buses travel in three conflicting directions and 60% of them travel on the north-bound approaches (San Pablo Avenue) and 40% on east-bound approaches (University Avenue). Bus headways vary from 10 to 30 minutes per each route. Information about the bus schedule is obtained from Almanda-Contra Costa Transit District, (2011). There are a number of bus stops at some distances from the intersection, however, their impacts on the intersection operation are ignored. The intersection's signal operates on a 4-phase cycle. The intersection flow ratio for evening peak hour, which is the analysis period in this study, is $Y = 0.73$. This value corresponds to a degree of saturation of

$X_c = 0.88$ for a cycle length of $C = 80$ seconds and lost time $L = 14$ seconds. This implies that during the evening peak hour traffic conditions are close to saturation.

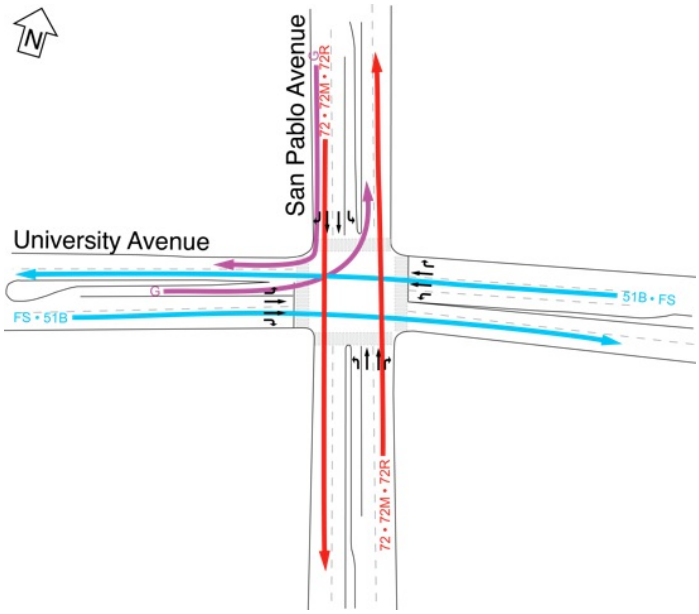

Figure 4.2: Layout and bus routes for the intersection of University and San Pablo Avenues, (Source: Christofa (2012)).

4.3 Results

This section presents the results of comparisons of emission-based optimization with vehicle-based optimization and person-based optimization. The comparison of the proposed emission based optimization with base case signal timings obtained from TRANSYT-7F are not presented since as shown in Table **??** both vehicle-based and emission-based optimizations are better than base-case scenario. Therefore, proving the advantage of emission-based scenario over vehicle-based and person-based scenarios justifies its advantage over base-case scenario, too.

Table 4.1: HC Emissions for $Y = 0.5$ for Intersection of Mesogion and Katechaki Avenues (Deterministic Arrival Tests)

	HC Emissions (g) (Auto)	HC Emissions (g) (Bus)	HC Emissions (g) (Total)
Scenario 0: TRANSYT-7F	72.51	11.86	84.37
Scenario 1: Vehicle-based	68.78	11.70	80.48
Scenario 2: Person-based	68.92	11.11	80.03
% Change in Emissions between Scenarios 0 and 1	-5.1%	-1.3%	-4.6%
% Change in Emissions between between Scenarios 0 and 2	-5.0%	-6.3%	-5.1%

Table 4.2: Person Delay for $Y = 0.5$ for Intersection of Mesogion and Katechaki Avenues (Deterministic Arrival Tests)

	Person Delay (pax-hours) (Auto)	Person Delay (pax-hours) (Bus)	Person Delay (pax-hours) (Total)
Scenario 0: TRANSYT-7F	28.61	8.38	37.00
Scenario 1: Vehicle-based	26.04	6.96	33.01
Scenario 2: Person-based	26.17	5.88	32.05
% Change in Emissions between Scenarios 0 and 1	-9.0%	-14.4%	-10.2%
% Change in Emissions between between Scenarios 0 and 2	-8.5%	-29.9%	-13.4%

4.3.1 Intersection of Mesogion and Katechaki Avenues

Figures 4.3 and 4.4 illustrate the improvement in HC emissions from vehicle-based and person-based optimization, respectively to the emission-based optimization for the deterministic arrival tests for autos, buses, as well as total emissions for a range of intersection flow ratios. Error bars show if the results are significant for 95% confidence interval. The Figures show that total HC emissions can be reduced by up to 2.5% and 4.4% compared to vehicle-based and person-based total HC emission levels, respectively. The lower the intersection flow ratio the higher the total emission reduction achieved. This occurs because at lower intersection flow ratios there

is more flexibility in the cycle to adjust green times to achieve substantial reductions in the emissions. Figure 4.3 also indicates that the majority of emission reductions is attributed to reducing bus emissions, which is a result of the higher emission rates for deceleration, cruising, and idling of buses compared to autos. This implies that buses are stopped fewer times. Therefore, some level of transit signal priority can be provided through emission-based optimization for HC compared to vehicle-based optimization. While bus emissions are reduced, emissions of autos is increased comparing the emission-based optimization to vehicle-based optimization (Figure 4.3). This happens because in emission-based optimization the weight of auto emissions in the objective function is reduced and it is given to transit vehicles. Therefore, we see reductions in bus emissions while increases in auto emissions. Comparing person-based optimization to emission-based optimization indicates that the change in bus emissions is negligible but a high reduction in auto emissions by up to 5.4% is observed (Figure 4.4). This Figure shows that auto emissions is reduced from person-based to emission-based optimization. This is because in emission-based optimization more weight is given to autos compared to person-based optimization.

The stochastic arrival test results for the same scenarios are shown in Figure 4.5 and 4.6. Due to the lack of perfect information in the simulation tests and the need to predict vehicle arrivals for both autos and buses, the percent changes for both comparisons (vehicle-based to emission-based and person-based to emission-based) reveal results that are not statistically significant as implied by the 95% confidence intervals shown on the graphs. Only for very light traffic conditions (Y=0.4) a comparison of the person-based to the emission-based scenario provides some benefits for overall emissions while increasing bus emissions.

At the same time total person delay decreases by up to 15% and bus person delay by up to 33% for low intersection flow ratios and deterministic arrival tests (Figure 4.7). When emission-based optimization is compared to person-based optimization

bus person delay can increase by up to 41% (Figure 4.8) indicating the higher effectiveness of person-based optimization in providing priority to buses. However, total person delay only experiences minor changes. Stochastic arrival tests reveal similar results but with lower bus person delay increases and in some cases not statistically significant percent change differences (Figure 4.9 and 4.10).

Performing deterministic arrival tests by minimizing NO_x emissions demonstrates improvements in total emissions from 3.6% to 6.7% and bus emissions from 4.6% to 7.6% depending on the flow ratio when comparing vehicle-based to emission-based optimization (Figure 4.11). For stochastic arrival tests emission-based optimization seems to be effective in minimizing total emissions for intersection flow ratios up to 0.5 (Figure 4.13). As before, stochasticity in arrivals affects the accuracy of auto and bus arrival predictions and the inaccuracies are higher at more congested traffic conditions. When comparing person-based to NO_x emission-based the differences in the results are not statistically significant (Figure 4.12 and 4.14). When comparing person delay from vehicle-based to NO_x emission-based optimization reductions in total person delay of up to 15% and bus person delay of up to 47% are observed for deterministic arrival tests (Figure 4.15) and lower percent changes of up to about 10.5% and 29% respectively for stochastic arrival tests (Figure 4.17).

A comparison of the person-based optimization with the NO_x emission-based optimization reveals that there are not statistically significant differences in person delays for both deterministic and stochastic arrival tests (Figure 4.16 and 4.18), which was also observed for the HC emission-based optimization. A comparison of the results between the NO_x emission-based and the HC emission-based optimization scenarios shows that higher total emission reductions and bus emissions reductions are achieved with the former since the emission rates for each operating mode for NO_x, especially for diesel buses are higher than those for HC.

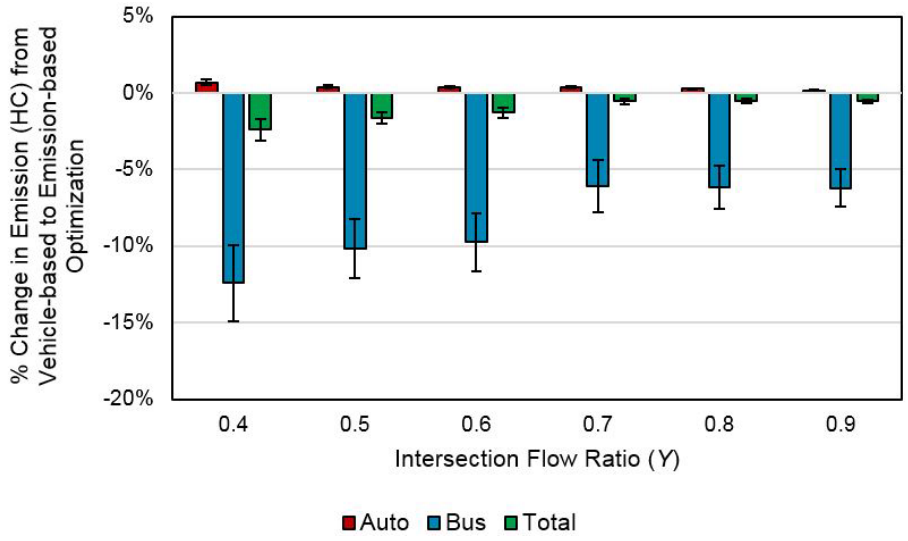

Figure 4.3: Percent change in HC emissions from vehicle-based to emission (HC)-based optimization for the intersection of Mesogion and Katechaki Avenues (deterministic arrival tests)

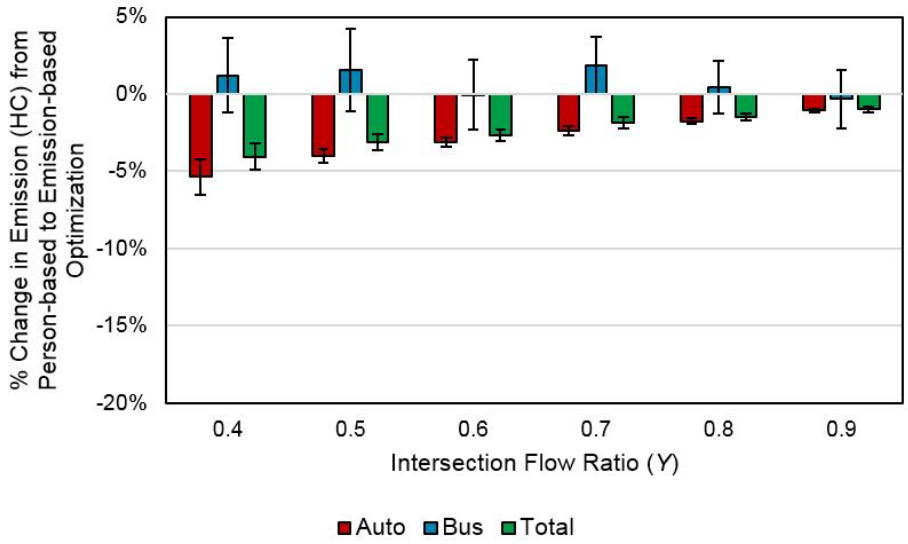

Figure 4.4: Percent change in HC emissions from person-based to emission (HC)-based optimization for the intersection of Mesogion and Katechaki Avenues (deterministic arrival tests)

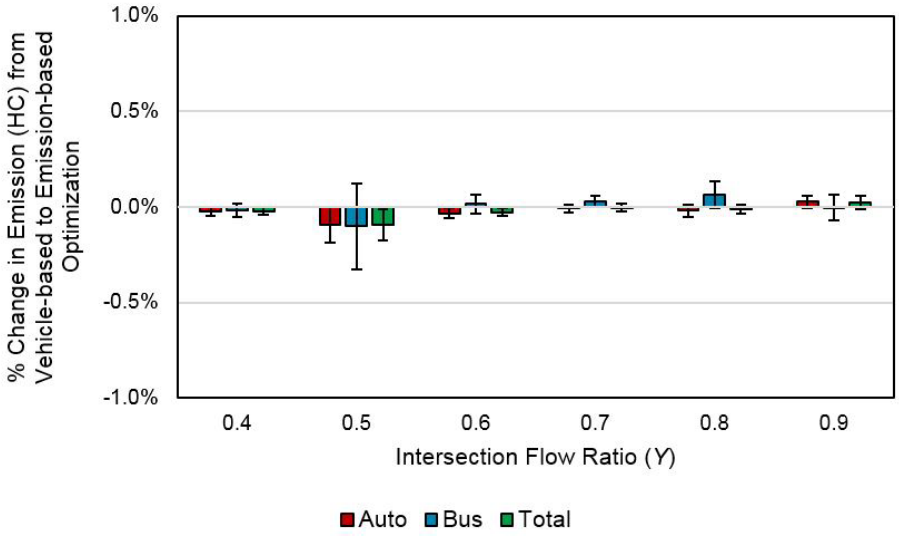

Figure 4.5: Percent change in HC emissions from vehicle-based to emission (HC)-based optimization for the intersection of Mesogion and Katechaki Avenues (stochastic arrival tests)

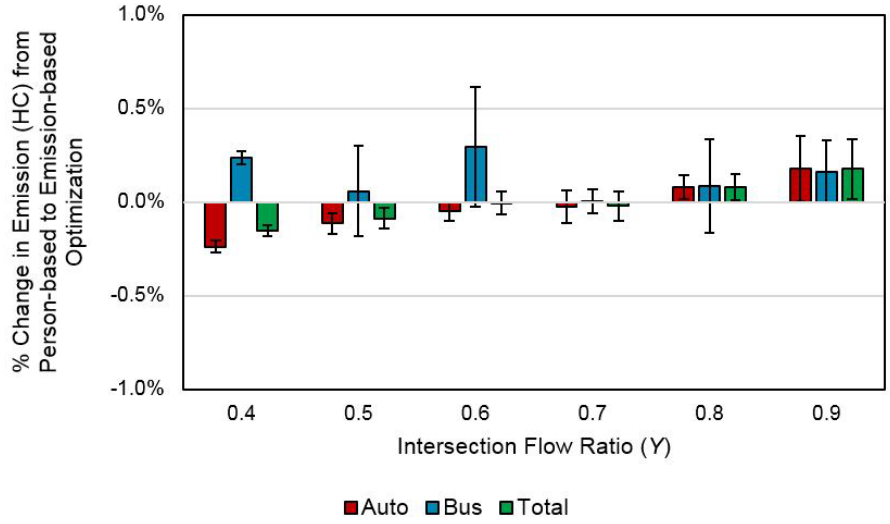

Figure 4.6: Percent change in HC emissions from person-based to emission (HC)-based optimization for the intersection of Mesogion and Katechaki Avenues (stochastic arrival tests)

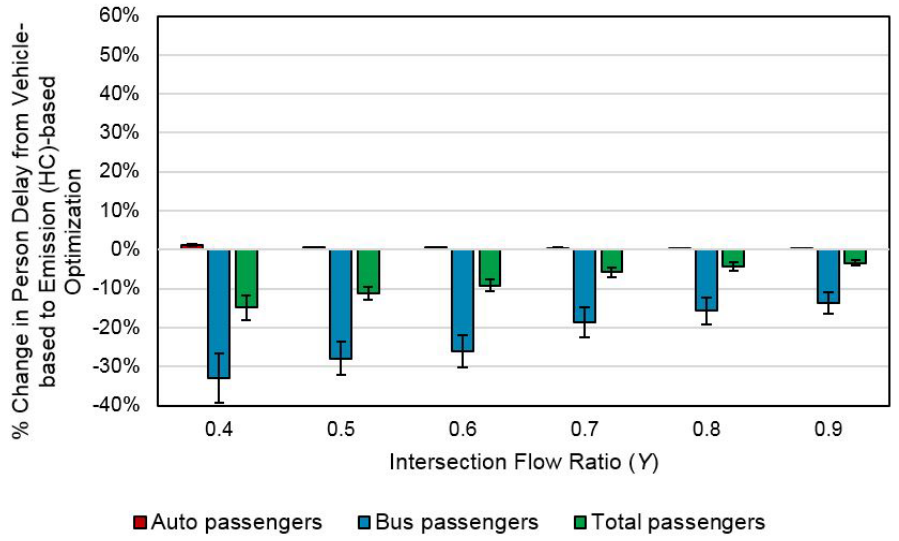

Figure 4.7: Percent change in person delay from vehicle-based to emission (HC)-based optimization for the intersection of Mesogion and Katechaki Avenues (deterministic arrival tests)

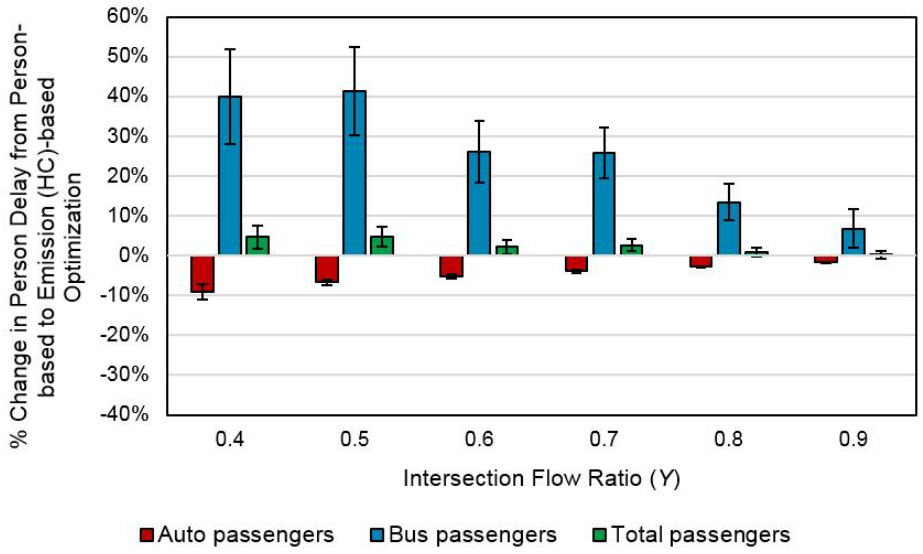

Figure 4.8: Percent change in person delay from person-based to emission (HC)-based optimization for the intersection of Mesogion and Katechaki Avenues (deterministic arrival tests)

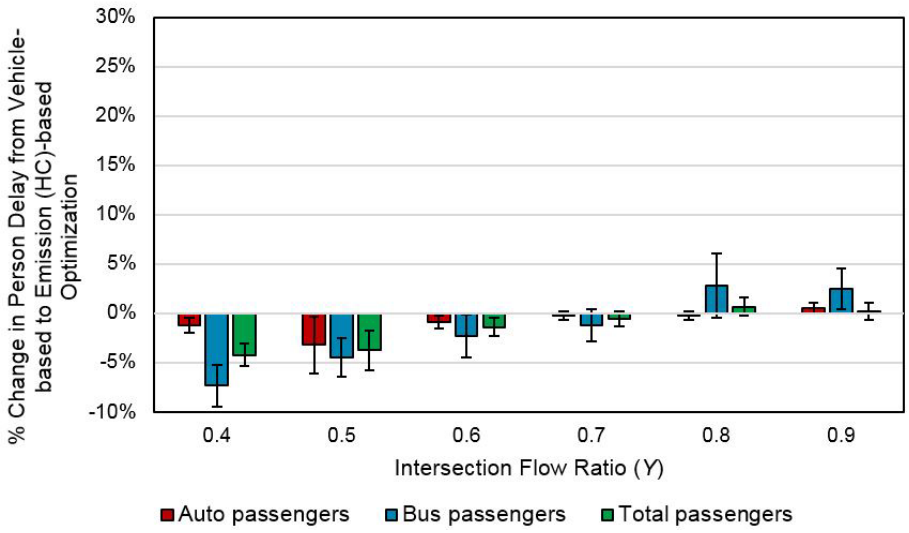

Figure 4.9: Percent change in person delay from vehicle-based to emission (HC)-based optimization for the intersection of Mesogion and Katechaki Avenues (stochastic arrival tests)

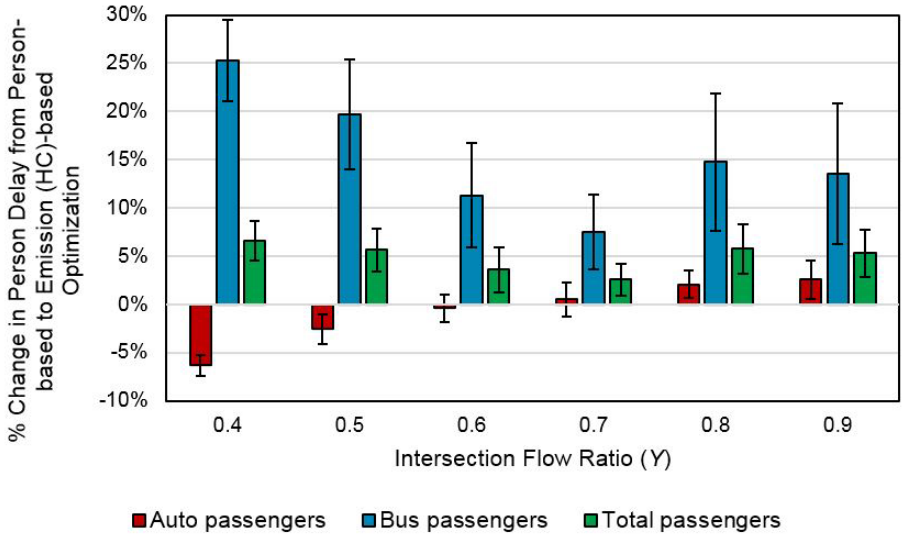

Figure 4.10: Percent change in person delay from person-based to emission (HC)-based optimization for the intersection of Mesogion and Katechaki Avenues (stochastic arrival tests)

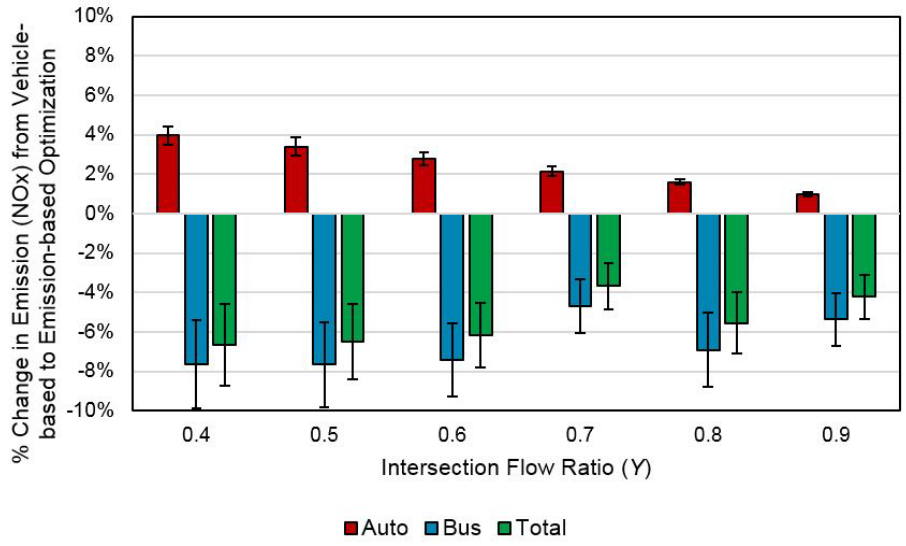

Figure 4.11: Percent change in NOx emissions from vehicle-based to emission (NOx)-based optimization for the intersection of Mesogion and Katechaki Avenues (deterministic arrival tests)

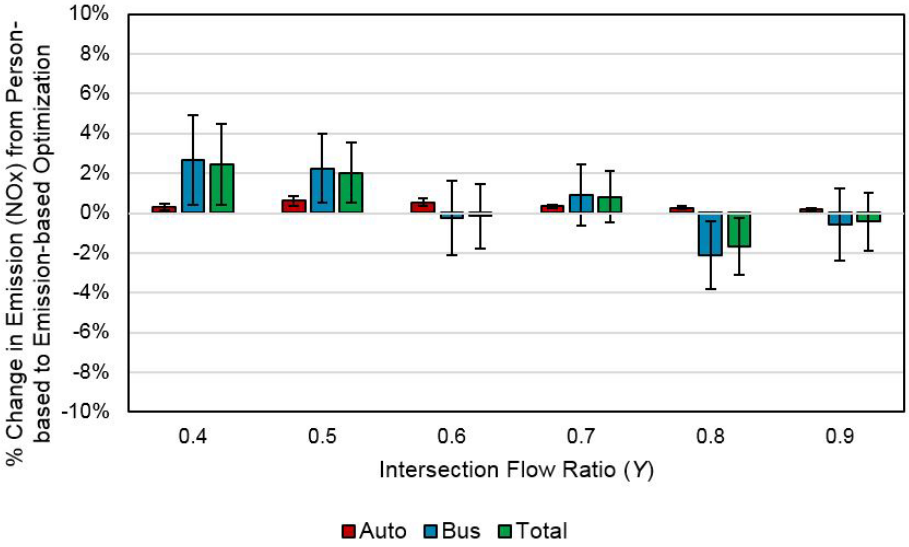

Figure 4.12: Percent change in NOx emissions from person-based to emission (NOx)-based optimization for the intersection of Mesogion and Katechaki Avenues (deterministic arrival tests)

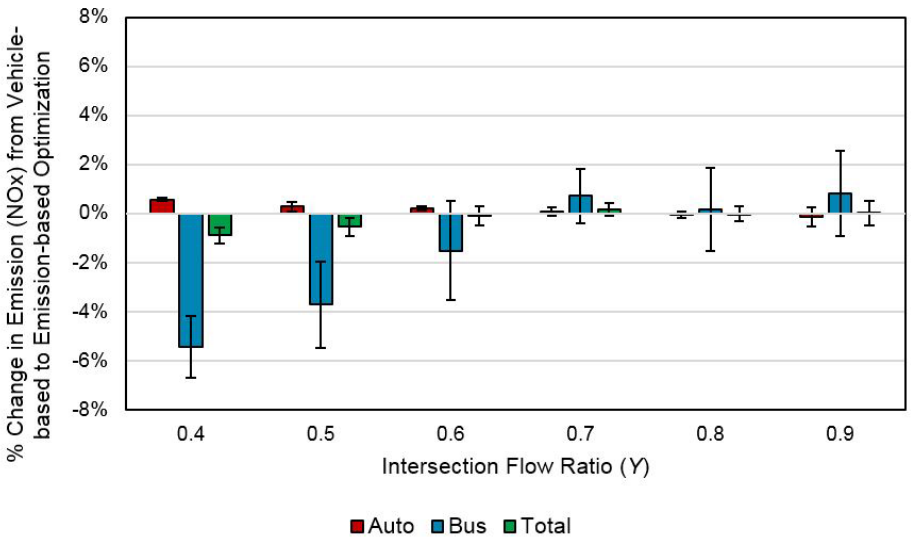

Figure 4.13: Percent change in NOx emissions from vehicle-based to emission (NOx)-based optimization for the intersection of Mesogion and Katechaki Avenues (stochastic arrival tests)

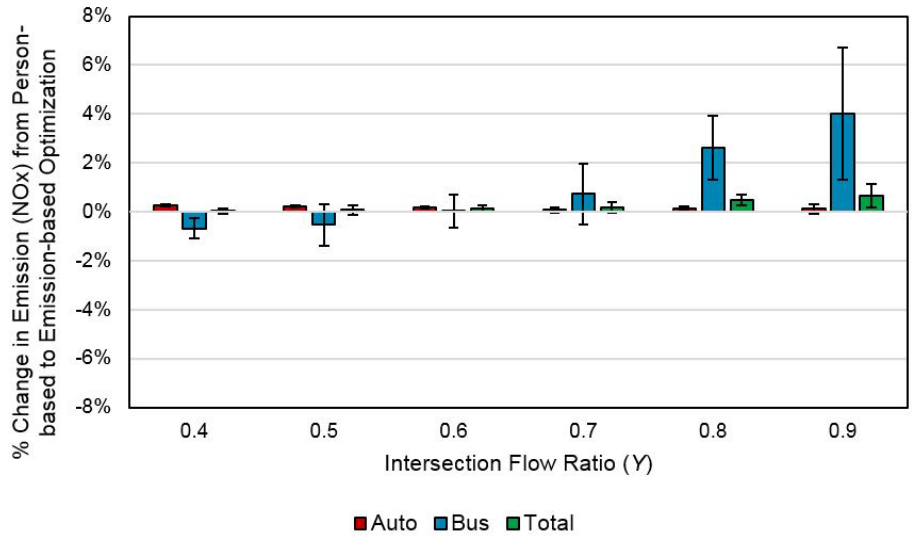

Figure 4.14: Percent change in NOx emissions from person-based to emission (NOx)-based optimization for the intersection of Mesogion and Katechaki Avenues (stochastic arrival tests)

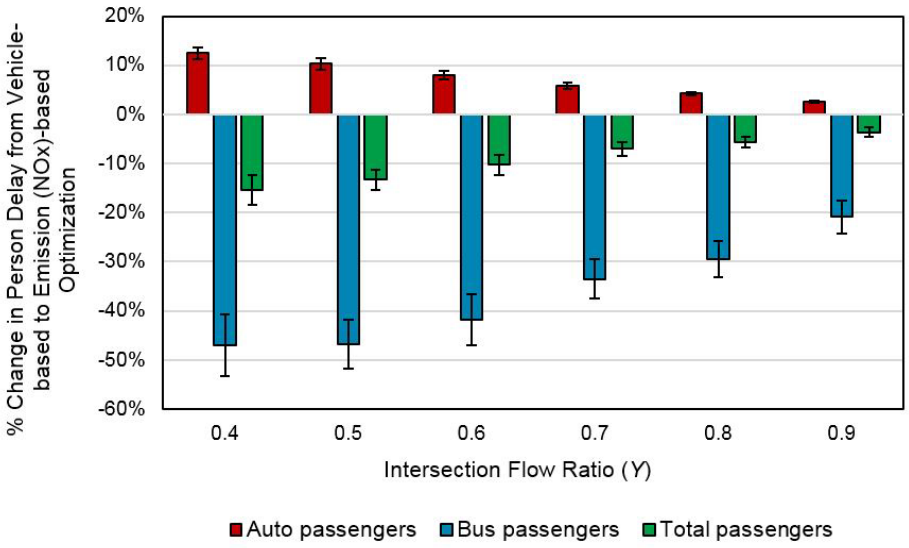

Figure 4.15: Percent change in person delay from vehicle-based to emission (NOx)-based optimization for the intersection of Mesogion and Katechaki Avenues (deterministic arrival tests)

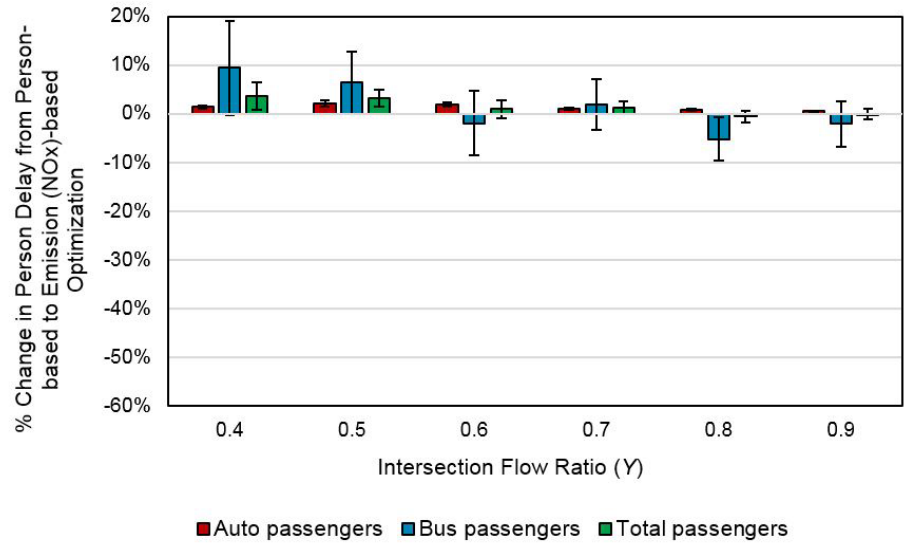

Figure 4.16: Percent change in person delay from person-based to emission (NOx)-based optimization for the intersection of Mesogion and Katechaki Avenues (deterministic arrival tests)

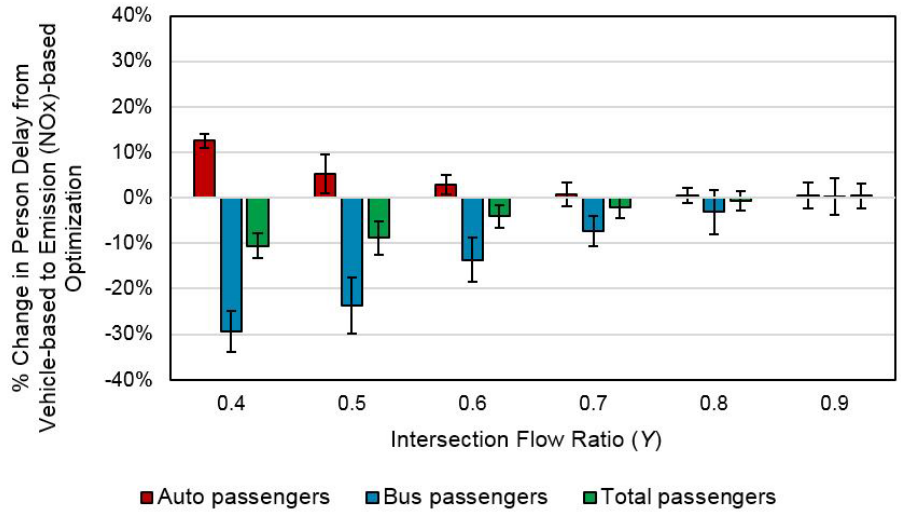

Figure 4.17: Percent change in person delay from vehicle-based to emission (NOx)-based optimization for the intersection of Mesogion and Katechaki Avenues (stochastic arrival tests)

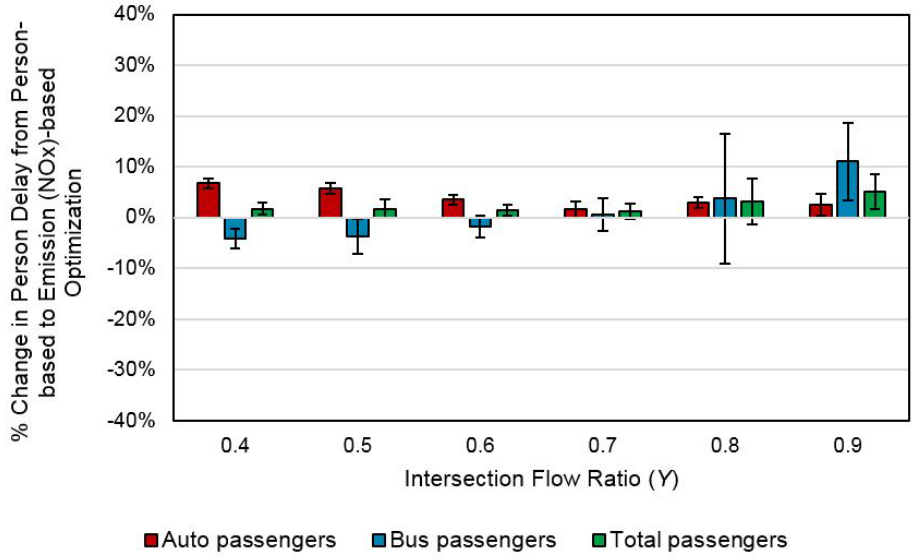

Figure 4.18: Percent change in person delay from person-based to emission (NOx)-based optimization for the intersection of Mesogion and Katechaki Avenues (stochastic arrival tests)

4.3.2 Intersection of University and San Pablo Avenues

Comparing the HC emissions resulting from the emission-based optimization to the vehicle-based and the person-based optimization, we observe minor or insignificant improvements in total emissions (Figures 4.19 and 4.20). However, bus emissions are reduced by up to 4.2% when comparing emission-based to vehicle-based optimization. Reductions observed in bus emissions are due to higher emission rates of buses. bus emissions do not improve significantly from person-based to emission-based optimization (Figure 4.20). This is because the specific emission rates used do not give a higher weight to buses compared to the weight that the number of passengers give them.

Figures 4.21 and 4.22 show the results of similar comparisons for emissions for stochastic arrival tests. As before, almost all results of stochastic tests are insignificant at the 95% confidence level due to lack of information about auto and bus arrival times.

Figure 4.23 shows up to 4% reduction in total person delay from vehicle-based to HC emission-based optimization. Also, bus person delay is reduced by up to 15% when these two scenarios are compared. Again, the reductions in bus person delay can be justified by the higher weight given to buses due to their higher emission rates. However, comparing both total person delay and bus person delay resulting from person-based to the ones from the emission-based optimization, we see minor increases, which is expected since the former directly optimizes person delay (Figure 4.24).

Similar tests have been performed for NO_x. Figure 4.27 shows that, total NO_x emissions are reduced by up to 3.5% for deterministic arrival tests. As shown in this figure a high portion of this reduction is due to the reduction in the NO_x emissions from buses. This happens because buses have relatively much higher NO_x emission rates compared to autos so they are provided with longer green times and

consequently, smoother vehicle operations. Comparing NO_x emissions resulting from person-based to the ones from the emission-based optimization, we do not see any significant differences (Figure 4.28).

The comparison of emissions from vehicle-based and person-based optimization to emission-based optimization shows no significant results for stochastic arrival tests (Figures 4.29 and 4.30). Due to the lack of perfect information, the performance of the emission-based signal control strategy is deteriorated in the stochastic arrival tests and we do not see any emission improvements.

Figures 4.31 and 4.32 show the comparison of person delay between NO_x emission optimization and vehicle-based and person-based optimization for deterministic arrival tests. Total person delay is reduced by up to 4% and bus delay by up to 18% when comparing vehicle-based and emission-based optimization for lower intersection flow ratios. However, the results of comparing person-based with emission-based optimization do not present any significant differences. Figures 4.33 and 4.34 show the same comparisons for stochastic arrival tests. As before, the performance of the system is deteriorated in stochastic arrival tests and almost all results are insignificant.

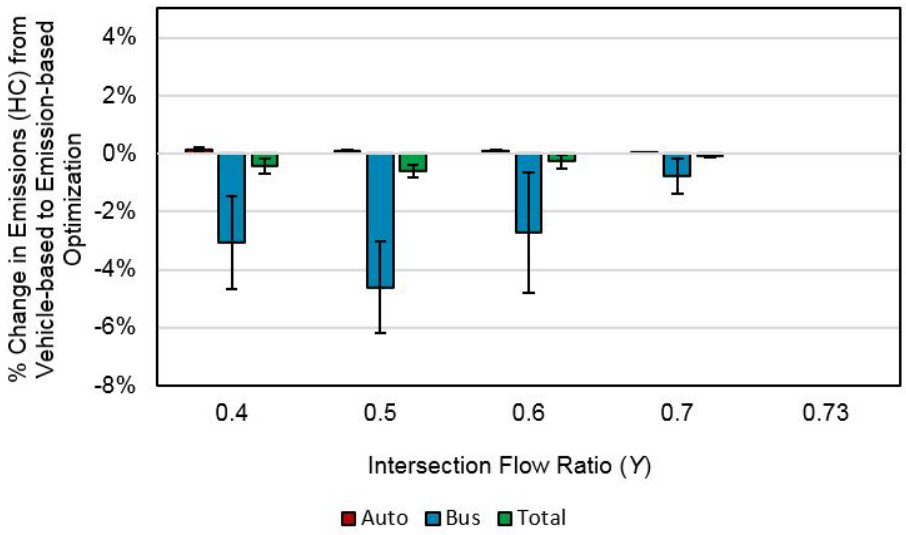

Figure 4.19: Percent change in HC emissions from vehicle-based to emission (HC)-based optimization for the intersection of University and San Pablo Avenues (deterministic arrival tests)

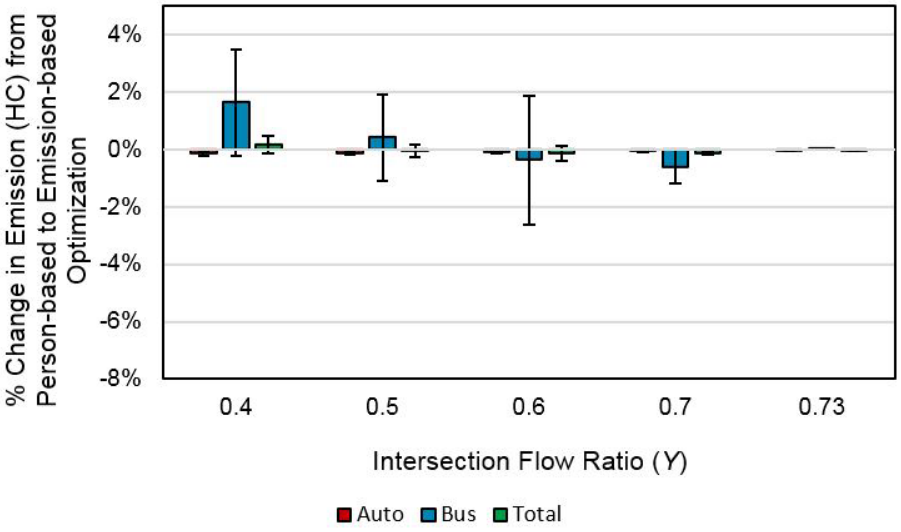

Figure 4.20: Percent change in HC emissions from person-based to emission (HC)-based optimization for the intersection of University and San Pablo Avenues (deterministic arrival tests)

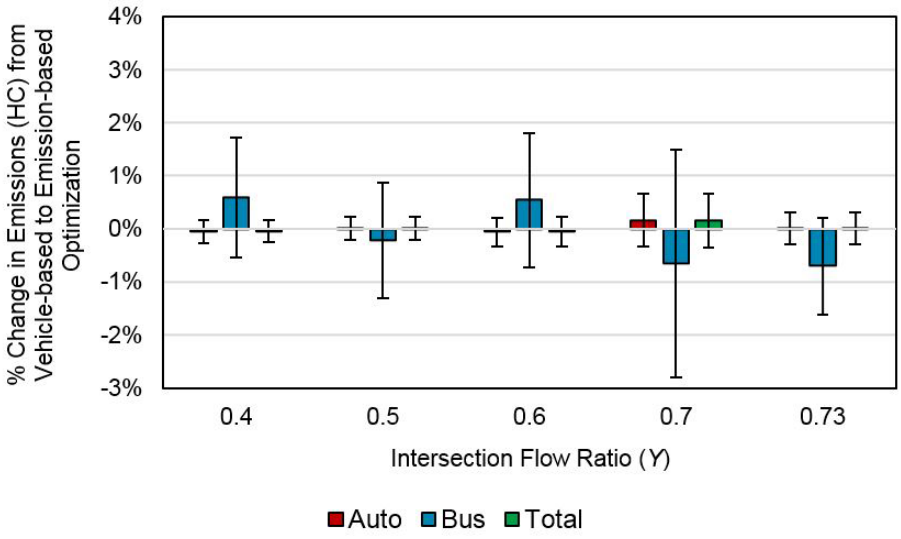

Figure 4.21: Percent change in HC emissions from vehicle-based to emission (HC)-based optimization for the intersection of University and San Pablo Avenues (stochastic arrival tests)

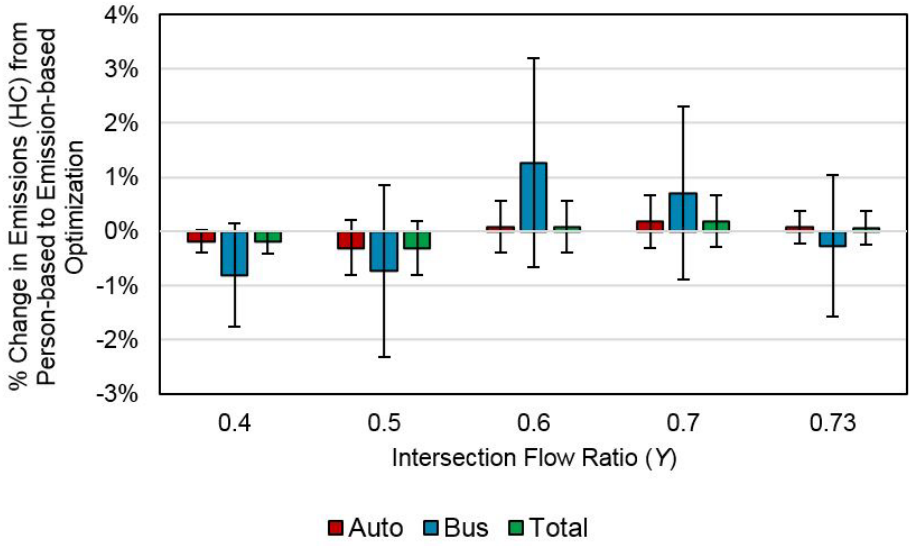

Figure 4.22: Percent change in HC emissions from person-based to emission (HC)-based optimization for the intersection of University and San Pablo Avenues (stochastic arrival tests)

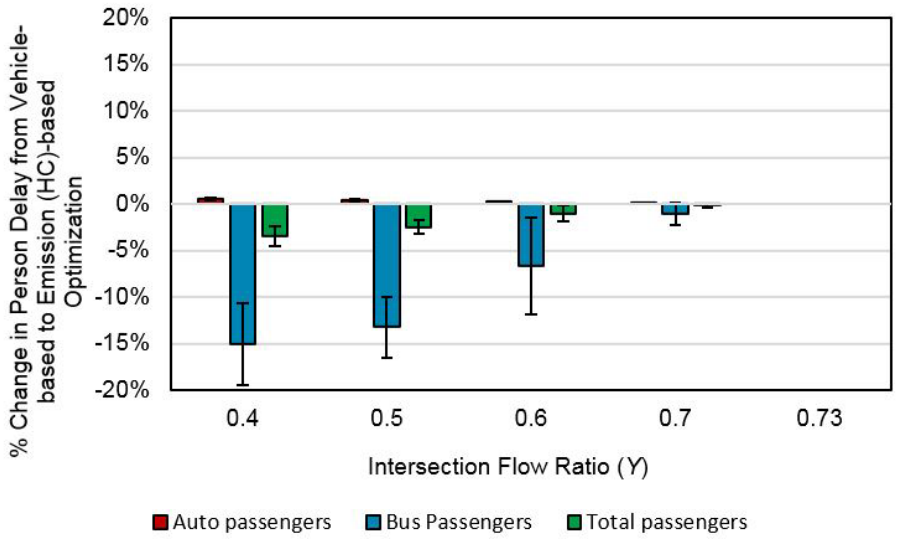

Figure 4.23: Percent change in person delay from vehicle-based to emission (HC)-based optimization for the intersection of University and San Pablo Avenues (deterministic arrival tests)

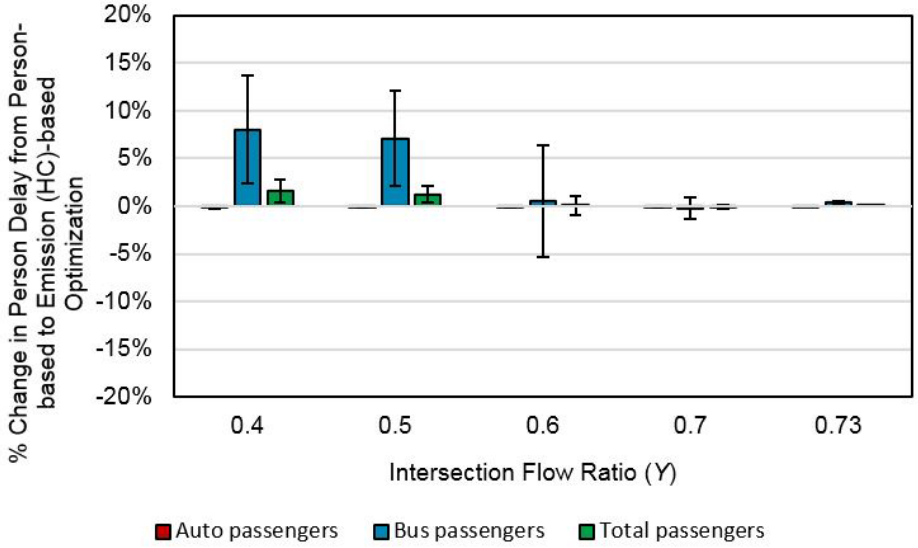

Figure 4.24: Percent change in person delay from person-based to emission (HC)-based optimization for the intersection of University and San Pablo Avenues (deterministic arrival tests)

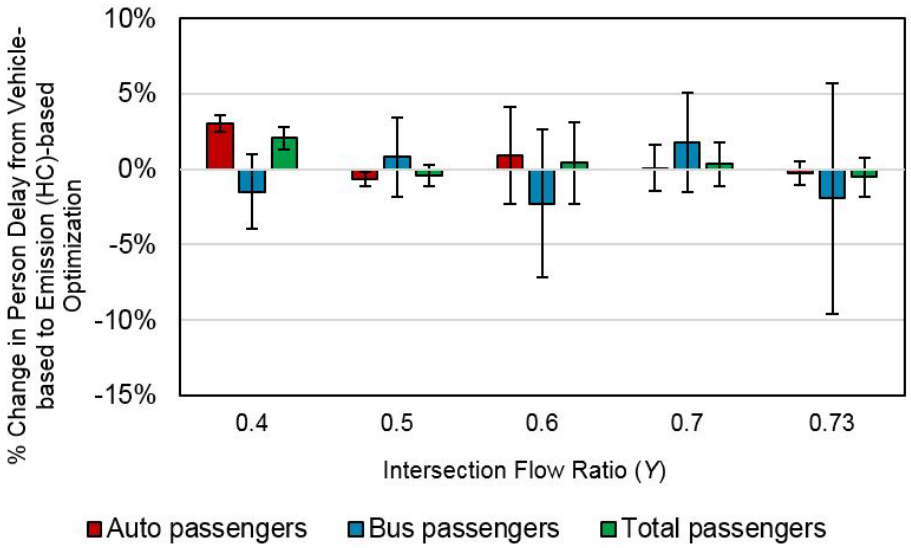

Figure 4.25: Percent change in person delay from vehicle-based to emission (HC)-based optimization for the intersection of University and San Pablo Avenues (stochastic arrival tests)

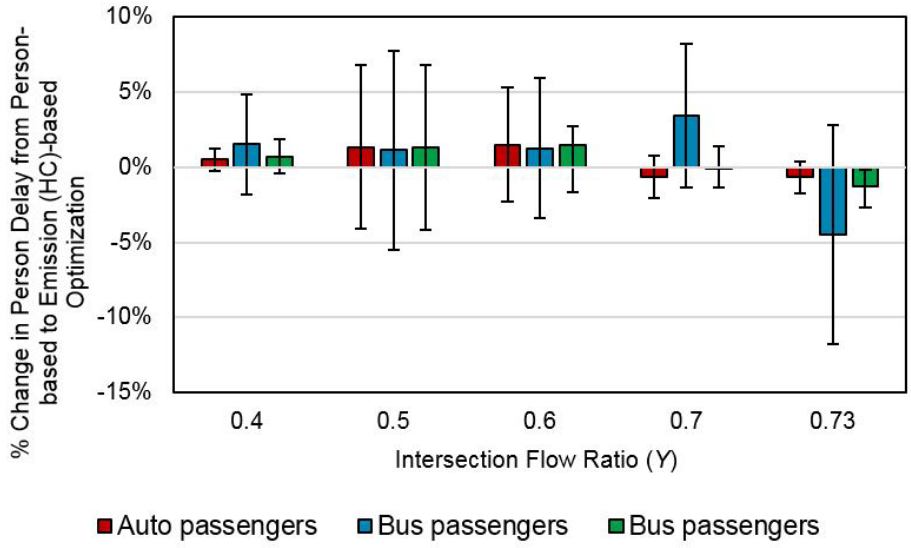

Figure 4.26: Percent change in person delay from person-based to emission (HC)-based optimization for the intersection of University and San Pablo Avenues (stochastic arrival tests)

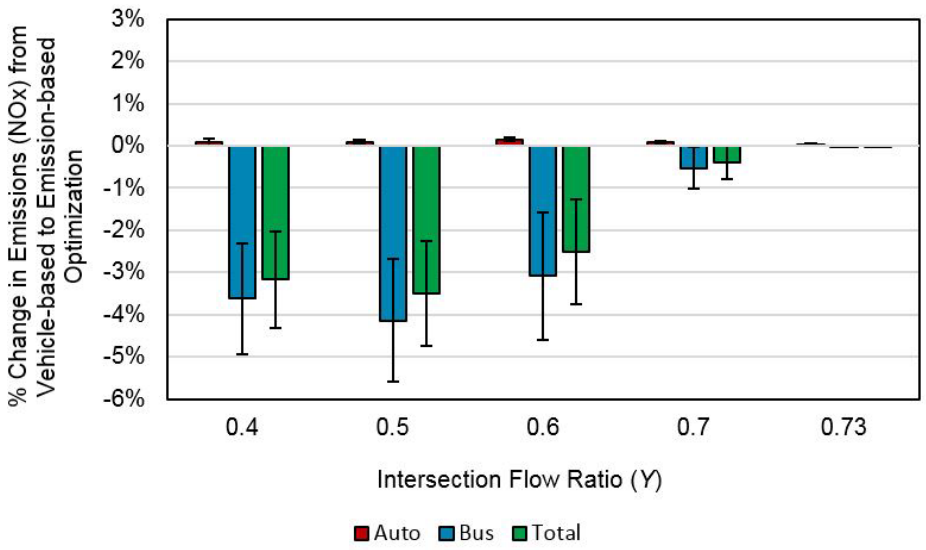

Figure 4.27: Percent change in NOx emissions from vehicle-based to emission (NOx)-based optimization for the intersection of University and San Pablo Avenues (deterministic arrival tests)

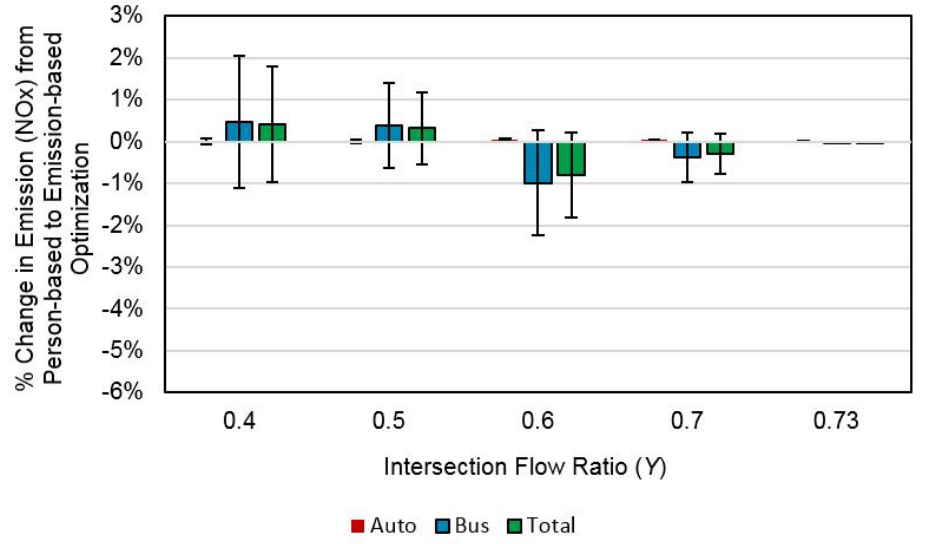

Figure 4.28: Percent change in NOx emissions from person-based to emission (NOx)-based optimization for the intersection of University and San Pablo Avenues (deterministic arrival tests)

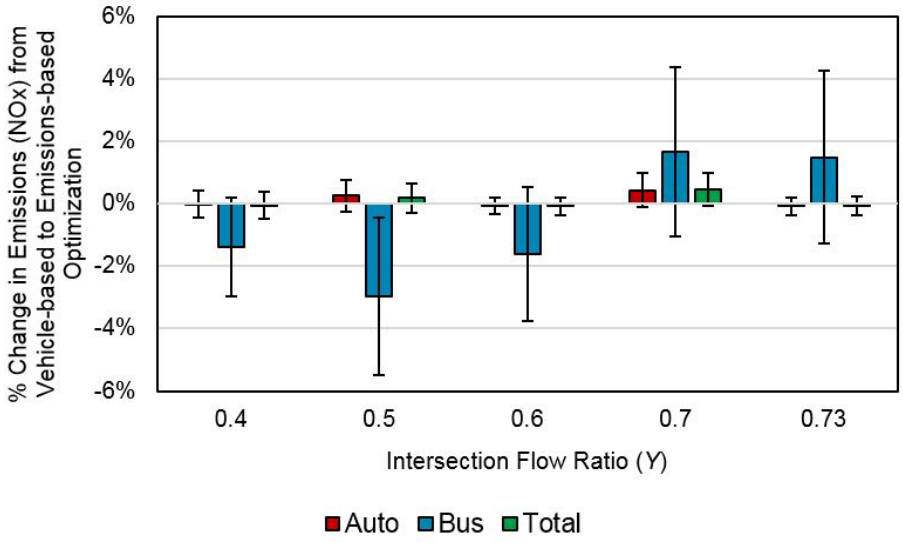

Figure 4.29: Percent change in NOx emissions from vehicle-based to emission (NOx)-based optimization for the intersection of University and San Pablo Avenues (stochastic arrival tests)

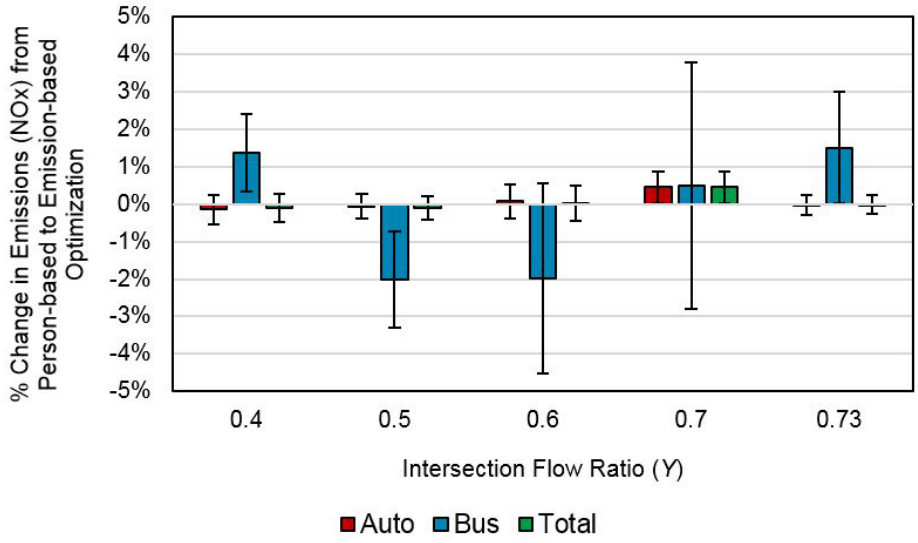

Figure 4.30: Percent change in NOx emissions from person-based to emission (NOx)-based optimization for the intersection of University and San Pablo Avenues (stochastic arrival tests)

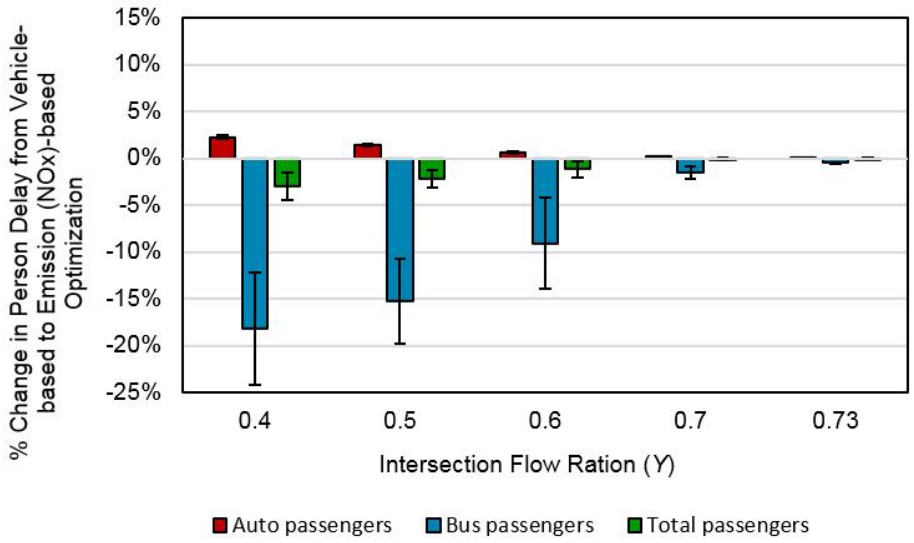

Figure 4.31: Percent change in person delay from vehicle-based to emission (NOx)-based optimization for the intersection of University and San Pablo Avenues (deterministic arrival tests)

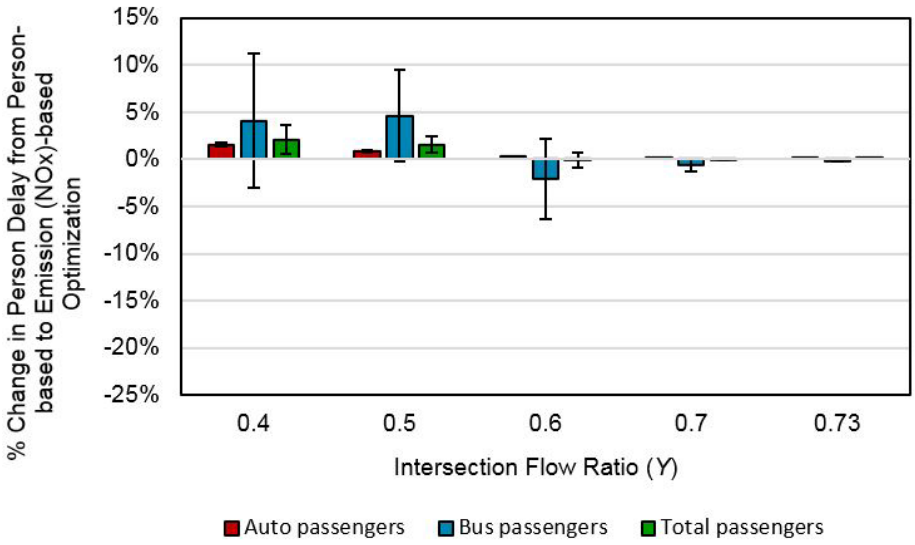

Figure 4.32: Percent change in person delay from person-based to emission (NOx)-based optimization for the intersection of University and San Pablo Avenues (deterministic arrival tests)

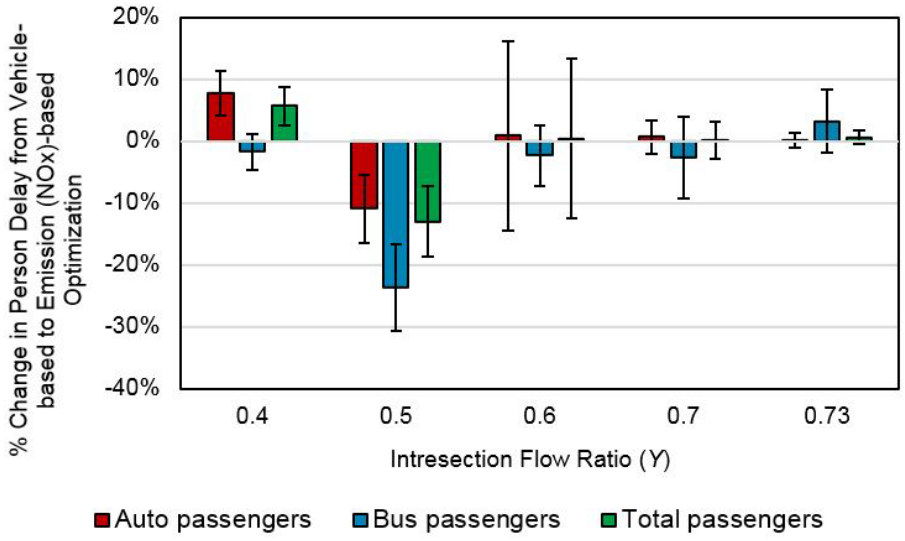

Figure 4.33: Percent change in person delay from vehicle-based to emission (NOx)-based optimization for the intersection of University and San Pablo Avenues (stochastic arrival tests)

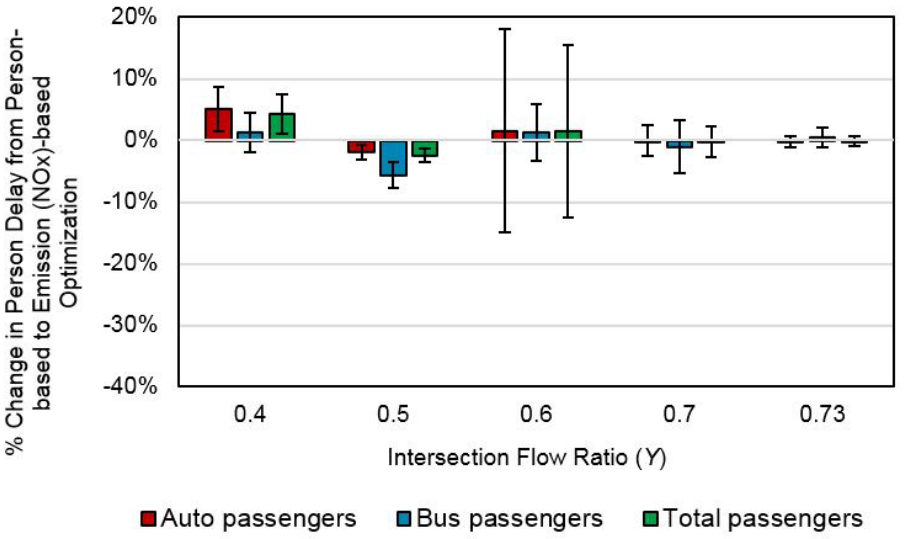

Figure 4.34: Percent change in person delay from person-based to emission (NOx)-based optimization for the intersection of University and San Pablo Avenues (stochastic arrival tests)

4.4 Summary of Findings

This research presents a real-time signal control system that minimizes total auto and transit vehicle emissions at an isolated intersection in undersaturated traffic conditions. The results of the evaulation of the proposed system using data from two real-world intersections in Athens, Greece and Berkeley, California indicate that in most cases the proposed system can reduce both total emissions and person delay compared to a vehicle-based optimization scenario. Additionally, transit person delay in the proposed scenario is considerably reduced compared to vehicle-based optimization, which can potentially result in improved transit ridership. The evaluation results also show that in most cases it can reduce total emissions when compared to the person-based optimization system.

A sensitivity analysis with respect to intersection flow ratio shows that the developed system is more effective in reducing total emissions and person delay for lower intersection flow ratios. As the flow ratio increases, the vehicle-based and emission-based signal optimization systems converge since the higher auto demand at nearly saturated conditions outweighs the weight given to transit vehicles due to their higher emission potential. In addition, the stochastic arrival tests performed indicate that the loss in the accuracy of auto and transit vehicle arrivals occurring in a more realistic environment deteriorates the performance of the emission and person-based optimization methods especially for traffic conditions close to saturation.

Comparing the results of two test sites, we observe smaller improvements in emissions for the same intersection flow ratio for the second intersection. As mentioned before the intersection of University and San Pablo Avenues features higher demand levels than the intersection of Mesogion and Katechaki Avenues for the same intersection flow ratio. Also, the intersection of University and San Pablo Avenues has a cycle length of 80 seconds with a total minimum green time of 34 seconds for all phases, and a lost time of 14 seconds. Therefore, the amount of time remained in each

cycle to be allocated to other phases is 32 seconds. For the intersection of Mesogion and Katechaki Avenues the cycle length of 120 seconds, the total minimum green time of 34 seconds, and lost time of 14 seconds result in a time of 72 seconds that can be allocated to different phases in each cycle. Therefore, there is much more flexibility in adjusting green times for the intersection of Mesogion and Katechaki Avenues compared to the intersection of University and San Pablo Avenues.

Note that the results are sensitive to the specific emission rates that are utilized and are expected to differ with different types of vehicles and will depend on the mix of those. In addition, while the presented results are for certain pollutants, HC and NO_x, the same methodology can be implemented utilizing emission rates per operating mode for any other pollutant.

CHAPTER 5

CONCLUSIONS

This research presents a real-time signal control system that minimizes total auto and transit vehicle emissions at an isolated intersection in undersaturated traffic conditions. The proposed system has been evaluated using the data of two real-wold intersections. The performance of this system has been compared to the performance of vehicle-based and person-based signal control systems in terms of emissions and person delay.

This chapter first presents a summary of research findings and the contributions of this study. Then next steps of improving and extending the model are presented.

5.1 Summary of Research Findings

Evaluating the proposed emission-based signal control systems by performing two types of deterministic and stochastic arrival tests on two tests sites, which are different in traffic conditions characteristics, we concluded that:

- emission-based signal control system can reduce both total emissions and person delay compared to the vehicle-based optimization optimization.
- the transit person delay resulted from the emission-based optimization is considerably reduced compared to the transit person delay obtained from the vehicle-based optimization, which can result in improved transit operations.
- in most cases the emission-based optimization can reduce total emissions when compared to the person-based optimization system.

- proposed system is more effective in reducing total emissions and person delay for lower intersection flow ratios. As the flow ratio increases, the vehicle-based and emission-based signal optimization systems converge.

- The loss in accuracy of auto and transit vehicle arrivals deteriorates the performance of the system in stochastic arrival tests

- Both the proposed emission-based and the person-based optimization that had been previously developed can be used to provide priority to transit vehicles and reduce overall emissions at intersections compared to commonly used vehicle-based optimization methods.

- person-based optimization is still the preferred signal control strategy when the goal is minimizing person delay, while emission-based optimization should be used when the goal is minimizing emissions.

- intersections with more spare time to be allocated to the different phases experience higher benefits in both person delay and emissions.

- the results of emissions are sensitive to the specific emissions rates that are utilized.

5.2 Contributions

There is literature on the impacts of signal control strategies on emissions. However, few studies have developed analytical models to estimate emissions for both autos and transit vehicles and even fewer have used them to develop signal control strategies to reduce emissions. In addition, none of the existing studies have explicitly optimize signal timings by minimizing emissions for both autos and transit vehicles. This study presents an analytical model to estimate emissions for both autos and transit vehicles at an isolated intersection, which operates at undersaturated traffic conditions. A

real-time signal control system that minimizes emissions at an intersection is also developed.

The proposed real-time control system uses real-time information on auto and transit vehicle arrivals and is able to adapt to changes in traffic conditions and provide optimal signal timings accordingly. Adjustments of signal timings to traffic conditions can potentially improve system efficiency. Furthermore, employing an analytical model to estimate emissions can result in reasonable computation times, which makes the use of this system feasible in the real-world.

Furthermore, the proposed system is likely to reduce delay experienced by transit vehicles. These vehicles have higher weights in the objective function of the optimization problem compared to autos due to their higher emissions rates. Therefore, they are provided with some level of priority to reduce their contributions to the emission production. This can potentially improve transit ridership and decrease congestion created by private autos in urban streets.

The signal control strategy that has been developed in this thesis can be a useful tool in improving the quality of life in urban areas by reducing emissions produced by autos and transit vehicles. In addition, depending on the traffic volumes, it is expected that public transportation users will benefit from this system and experience lower travel times.

5.3 Future work

The real-time signal control system can be extended in a number of ways as follows:

- As we observed in the stochastic arrival test, the performance of the system gets deteriorated due to lack of perfect information on vehicle arrival flows and times. Therefore, we plan to improve the performance of the system by designing a better vehicle arrival prediction algorithm.

- Due to the assumptions we made in order to estimate vehicular emissions, the proposed system works for undersaturated traffic conditions, which is usually not the case during peak hours. Thus, developing an analytical model to estimate emissions of autos and transit vehicles for oversaturated traffic conditions is one of the future steps of this research.

- Accounting for the upstream and downstream intersections while optimizing signal timings is very important since there are a lot of signalized arterials in urban areas, which can benefit from an emission-based signal control system. As a result, we plan to extend our developed emission-based signal control system to a signalized arterial.

- While minimizing emissions is imperative at signalized intersections, it is also necessary to consider the effects of a signal control system on person delay, which is of the most important performance measures at signalized intersections. The next step of this study is developing a real-time signal control system to reduce both emissions and person delay at signalized intersections.

BIBLIOGRAPHY

Highway Capacity Manual, 3rd edition. Transportation Research Board Special Report 209, National Research Council, Washington, DC, 2000.

AC Transit. Alameda-Contra Costa Transit District. http://www.actransit.org, Accessed August 2011.

Kyoungho Ahn, Hesham Rakha, Antonio Trani, and Michel Van Aerde. Estimating vehicle fuel consumption and emissions based on instantaneous speed and acceleration levels. *Journal of Transportation Engineering*, 128(2):182–190, 2002.

Song Bai, Douglas Eisinger, and Deb Niemeier. Moves vs. emfac: A comparison of greenhouse gas emissions using los angeles county. In *Transportation Research Board 88th Annual Meeting, Paper*, pages 09–0692, 2009.

Matthew Barth and Kanok Boriboonsomsin. Real-world carbon dioxide impacts of traffic congestion. *Transportation Research Record: Journal of the Transportation Research Board*, 2058(1):163–171, 2008.

Matthew Barth, Feng An, Theodore Younglove, C Levine, G Scora, Marc Ross, and Thomas Wenzel. *Development of a comprehensive modal emissions model*. National Cooperative Highway Research Program, Transportation Research Board of the National Academies, 2000.

William R. Black. *Sustainable Transportation: Problems and Solutions*. The Guilford Press, New York, London, 1942.

Robert Chamberlin, Ben Swanson, Eric Talbot, Jeff Dumont, and Stephen Pesci. Analysis of moves and cmem for evaluating the emissions impact of an intersection control change. In *Transportation Research Board 90th Annual Meeting*, number 11-0673, 2011.

Kun Chen and Lei Yu. Microscopic traffic-emission simulation and case study for evaluation of traffic control strategies. *Journal of Transportation Systems Engineering and Information Technology*, 7(1):93–99, 2007.

Xumei Chen, Lei Yu, Yi Qi, Xin Li, and Xiaofei Sun. Analysis of the effects of signal related parameters on the intersection speed profiles: an alternative perspective to estimate emission for signalized intersections. In *Transportation Research Board 94th Annual Meeting*, number 15-2102, 2015.

Eleni Christofa. *Traffic Signal Optimization with Transit Priority: A Person-Based Approach*. PhD thesis, University of California Berkeley, 2012.

Eleni Christofa, Ioannis Papamichail, and Alexander Skabardonis. Person-based traffic responsive signal control optimization. *Intelligent Transportation Systems, IEEE Transactions on*, 14(3):1278–1289, 2013.

Clean Air Technologies International, Inc. OEM 2100. http://globalmrv.com/, Accessed February 2015.

Robert Jay Dilger. State and Local Government Officials' Perspectives on Intergovernmental Relationships in Surface Transportation Policy: 1987 and 2001. *Publius: The Journal of Federalism*, 32(1):65–85, 2002.

EPA. Health. EPA. Environmental Protection Agency. http://www.epa.gov/oaqps001/nitrogenoxides/health.html, Accessed February 2015.

Christodoulos A Floudas. *Nonlinear and mixed-integer optimization: fundamentals and applications*. Oxford University Press, 1995.

Henry Christopher Frey, Nagui Rouphail, Alper Unal, and James Colyar. Emissions and traffic control: an empirical approach. In *CRC On-Road Vehicle Emissions Workshop, San Diego, CA*, 2000.

Henry Christopher Frey, Nagui M Rouphail, A Unal, and James D Colyar. Measurement of on-road tailpipe co, no, and hydrocarbon emissions using a portable instrument. In *Proceedings, Annual Meeting of the Air & Waste Management Association*. Citeseer, 2001a.

Henry Christopher Frey, Nagui M Rouphail, Alper Unal, and JD Colyar. Emissions reduction through better traffic management: An empirical evaluation based upon on-road measurements. Technical report, 2001b.

Henry Christopher Frey, Alper Unal, Nagui M Rouphail, and James D Colyar. On-road measurement of vehicle tailpipe emissions using a portable instrument. *Journal of the Air & Waste Management Association*, 53(8):992–1002, 2003.

Henry Christopher Frey, Nagui M Rouphail, and Haibo Zhai. Speed-and facility-specific emission estimates for on-road light-duty vehicles on the basis of real-world speed profiles. *Transportation Research Record: Journal of the Transportation Research Board*, 1987(1):128–137, 2006.

Rui Guo and Yu Zhang. The relationship between mobility and environmental externalities at signalized intersections. In *Transportation Research Board 93rd Annual Meeting*, number 14-3347, 2014.

Bruce. Hellinga, M. A. Khan, and L. Fu. Analytical emission models for signalized arterials. *Proceedings of the Canadian Society of Civil Engineers 3rd Transportation Specialty Conference held in London, Ontorio, June 7-10*, 2000.

John Koupal, Mitch Cumberworth, Harvey Michaels, Megan Beardsley, and David Brzezinski. Design and implementation of moves: Epas new generation mobile source emission model. *Ann Arbor*, 1001:48105, 2003.

Chen Kun and Yu Lei. Microscopic traffic-emission simulation and case study for evaluation of traffic control strategies. *Journal of Transportation Systems Engineering and Information Technology*, 7(1):93–99, 2007.

Pengfei Li, Pitu Mirchandani, and Xuesong Zhou. Simulation-based traffic signal optimization to minimize fuel consumption and emission: A lagrangian relaxation approach. *Transportation Research Board*, 2015.

OASA. Search Route. www.oasa.gr, 2010. URL `www.oasa.gr`.

Toshihiko Oda, Masao Kuwahara, and Satoshi Niikura. Traffic signal control for reducing vehicle carbon dioxide emissions on an urban road network. *Proc. 11th World Congr. ITS*, pages 1–8, 2004.

Hesham Rakha and Yonglian Ding. Impact of stops on vehicle fuel consumption and emissions. *Journal of Transportation Engineering*, 129(1):23–32, 2003.

Hesham Rakha, A Medina, H Sin, F Dion, M Van Aerde, and J Jenq. Traffic signal coordination across jurisdictional boundaries: Field evaluation of efficiency, energy, environmental, and safety impacts. *Transportation Research Record: Journal of the Transportation Research Board*, 1727(1):42–51, 2000a.

Hesham Rakha, Michel Van Aerde, K Ahn, and Antonio A Trani. Requirements for evaluating traffic signal control impacts on energy and emissions based on instantaneous speed and acceleration measurements. *Transportation Research Record: Journal of the Transportation Research Board*, 1738(1):56–67, 2000b.

Hesham Rakha, Youn-Soo Kang, and François Dion. Estimating vehicle stops at undersaturated and oversaturated fixed-time signalized intersections. *Transportation Research Record: Journal of the Transportation Research Board*, 1776(1):128–137, 2001.

Hesham Rakha, Kyoungho Ahn, Ihab El-Shawarby, and Sebong Jang. Emission model development using in-vehicle on-road emission measurements. In *Annual Meeting of the Transportation Research Board, Washington, DC*, volume 2, 2004a.

Hesham Rakha, Kyoungho Ahn, and Antonio Trani. Development of vt-micro model for estimating hot stabilized light duty vehicle and truck emissions. *Transportation Research Part D: Transport and Environment*, 9(1):49–74, 2004b.

Nagui M. Rouphail, H. Christopher Frey, James D. Colyar, and Alper Unal. Vehicle emissions and traffic measures: exploratory analysis of field observations at signalized arterials. In *80th Annual Meeting of the Transportation Research Board, Washington, DC*, 2001.

Kathy Salamati, Nagui M. Rouphail, H. Christopher Frey, Bin Liu, and Bastian J. Schroeder. A simplified method for comparing emissions at roundabouts and signalized intersections. *Submitted for Consideration for Presentation and Publication at the 94th TRB Annual Meeting*, 2015.

Rooholamin Shabihkhani and Eric J Gonzales. Analytical model for vehicle emissions at a signalized intersection: Integrating traffic and microscopic emissions models. In *Transportation Research Board 92nd Annual Meeting*, number 13-5208, 2013.

Alexander Skabardonis, Nikolas Geroliminis, and Eleni Christofa. Prediction of vehicle activity for emissions estimation under oversaturated conditions along signalized arterials. *Journal of Intelligent Transportation Systems*, 17(3):191–199, 2013.

Fotis G Stathopoulos and Robert B Noland. Induced travel and emissions from traffic flow improvement projects. *Transportation Research Record: Journal of the Transportation Research Board*, 1842(1):57–63, 2003.

Aleksandar Stevanovic, Jelka Stevanovic, Kai Zhang, and Stuart Batterman. Optimizing traffic control to reduce fuel consumption and vehicular emissions. *Transportation Research Record: Journal of the transportation research board*, 2128(1): 105–113, 2009.

Stan Teply, DI Allingham, DB Richardson, and BW Stephenson. Canadian capacity guide for signalized intersections. 1995.

TSS. *Aimsun users manual v6.1.* Transport Simulation Systems, Barcelona, Spain, 2010.

Alper Unal, Nagui M Rouphail, and H Christopher Frey. Effect of arterial signalization and level of service on measured vehicle emissions. *Transportation Research Record: Journal of the Transportation Research Board*, 1842(1):47–56, 2003.

Charles E Wallace, KG Courage, DP Reaves, GW Schoene, and GW Euler. Transyt-7f user's manual. Technical report, 1984.

Yunpeng Wang, Dong Guo, Shiwu Li, Yu Wang, and Zu Li. Signal timing optimization simulation on urban road intersection based on vehicle emissions. In *Proceedings of the 8th International Conference of Chinese Logistics and Transportation ProfessionalsLogistics*, pages 4762–4767, 2008.

Solomon K Zegeye, Bart De Schutter, Hans Hellendoorn, and Ewald Breunesse. Model-based traffic control for balanced reduction of fuel consumption, emissions, and travel time. In *Proceedings of the 12th IFAC Symposium on Transportation Systems*, pages 149–154, 2009.

Haibo Zhai, H Christopher Frey, and Nagui M Rouphail. A vehicle-specific power approach to speed-and facility-specific emissions estimates for diesel transit buses. *Environmental science & technology*, 42(21):7985–7991, 2008.

Yingying Zhang, Chen Xumei, Xiao Zhang, Song Guohua, Hao Yanzhao, and Yu Lei. Assessing effect of traffic signal control strategies on vehicle emissions. *Journal of Transportation Systems Engineering and Information Technology*, 9(1):150–155, 2009.